



Evaluation of satellite-based rainfall estimates over the IGAD region of Eastern Africa

Paulino Omoj Omay^{1,2} · Nzioka J. Muthama¹ · Christopher Oludhe¹ · Josiah M. Kinama¹ · Guleid Artan² · Zachary Atheru²

Received: 14 February 2024 / Accepted: 11 February 2025

© The Author(s) 2025

Abstract

Satellite precipitation (rainfall) products have become increasingly valuable in the delivery of climate services in recent years, particularly in Africa, where the network of synoptic stations has been gradually declining. The Satellites-based Rainfall Estimates (SREs) are estimates and measurements; thus, accuracy is of major concern. This study gives a detailed long-term comparison and evaluation of nine (9) SREs from 2001 to 2020 over East Africa. The study used 105 rain gauge observations and gridded 9 SRE products. The statistical methods such as rainfall totals, annual cycle, 24 continuous, categorical, and volumetric metrics, scatter plots, the Cumulative Distribution Function (CDF), and colored code portraits were employed to assess the temporal and spatial patterns of SREs performance. The evaluation was conducted at each 105-rain gauge spatially and in five sub-regions for different metrics and performance comparisons during March–May (MAM), June–September (JJAS), and October–December (OND). Our findings demonstrate that relying on a single metric for validating the performance of SREs is not sufficient. Instead, it is necessary to utilize multiple metrics to assess rainfall performance, especially in areas with complex topography such as mountains and diverse climatic zones. The spatial patterns of validation of nine SREs showed CMORPH RT, CHIRPS v2.0, CPC-RFEv2, and GPM-IMERG are the top four best-performing SREs. The CMORPH RT emerged the best-performing SRE, followed by CHIRPS v2.0. Also, the satellite products tend to slightly underestimate the rainfall throughout the region. Geographically, SREs performed well over highlands compared to desert and semi-arid regions, while seasonally, the accuracy of SRE was lower over JJAS compared to MAM and OND. This study further demonstrated that the density and distribution of synoptic stations (rain gauges) in a country play a significant role in the accuracy of validation. These findings shows that SREs play complementary roles in the accurate monitoring and analysis of precipitation and provide comprehensive coverage, especially in remote areas where ground-based measurements are sparse. These findings serve as guidance to climate service providers and end-users on how to select suitable alternative rainfall datasets for different applications and feedback to the algorithm developers to improve the SRE products.

1 Introduction

East Africa is highly exposed to the effects of change and variability of climate, especially changes in rainfall events (Ongoma, et al. 2018). The high vulnerability is attributable

to climate-sensitive socioeconomic activities, which rely on rainfall in nearly every case (Anyah and Qiu 2012). The livelihood activities in East Africa are highly vulnerable to extreme rainfall variability and change due to their sensitivity to climate (Taylor et al. 2013; Ongoma and Chen 2017). Real-time rainfall Estimates are critical for the scientific research and significantly impact economic activity in various sectors by providing critical information for decision-making, risk management, and operational planning (Tarnavsky & Bonifacio 2020). Rainfall estimates for a week or ten days (dekad) may be utilized to detect periods of less precipitation that may lead to crop deficiencies, but estimates for an hourly and daily time-step are required for driving rainfall run-off models used for flood forecasting, flash floods and river management.

Responsible Editor: Silvia Trini-Castelli.

✉ Paulino Omoj Omay
paulinoomay@gmail.com

¹ Department of Earth and Climate Sciences, Faculty of Science & Technology, University of Nairobi, Nairobi, Kenya

² IGAD Climate Prediction and Application Centre (ICPAC), Nairobi, Kenya

Long-term satellite precipitation records are crucial for studying climate trends, variability, and change, drought patterns and trends, and supporting agricultural planning and water resource management. The timeline and key missions of satellite observations date back to about 1979. The Nimbus-7 and Defense Meteorological Satellite Program (DMSP) were the early missions in the 1970s–1980s (Schwartz 2004), followed by enhanced capabilities in the 1990s such as the Tropical Rainfall Measuring Mission (TRMM) in the period between 1997 and 2015 (Huffman et al. 2007). This mission was a major milestone in precipitation observation, providing detailed measurements of tropical rainfall using a combination of radar and microwave sensors. In the 2000s, the capabilities of satellite remote sensing expanded with missions such as the Advanced Microwave Scanning Radiometer-EOS (AMSR-E) in 2002 (Kawanishi et al. 2003), and CloudSat and CALIPSO in 2006. In the 2010s, there was further integration and innovation with missions such as the Global Precipitation Measurement (GPM) in 2014, and the Integrated Multi-satellite Retrievals for GPM (IMERG) (Smith et al. 2007), which integrates data from multiple satellite platforms to produce high-resolution precipitation estimates on a global scale.

Since 2007, the researcher, climate and applications centers has made significant strides toward renovating Satellites-based Rainfall Estimates (SREs) inputs and outputs into precise, reliable, and timely observations, as well as generating rainfall products for climate services operations that are readily available for a wide range of socioeconomic applications. Weather and climate research, nowcasting products that improve Numerical Weather Prediction(NWP), water and energy, agriculture and food security, health and nutrition, and many more applications can benefit from Satellites-based products. The SREs products are currently regarded as alternative to the ground rain gauge observations (Cattani et al., 2016, Dinku et al. 2018a, b, Ayehu et al. 2018, Levizzani et al. 2020). Also, information from SREs form a vital tool for a variety of applications that enhance disaster risk reduction, early warning and response, and save lives.

The capacity to validate SREs products largely reliant on the presence of a reliable benchmark rain gauge dataset. However, in underdeveloped nations, the density and distribution of rain gauges is very low. in Africa, Asia, and South America. This may jeopardize the processes and the reliability of the final conclusions. Some researchers have attempted to employ alternate methodologies for validating SREs in the absence of ground-gauge observations to address the issue of a nonexistent or less rain gauge to validate SREs. Triple Collocation Analysis (TCA) is one of these techniques. The earliest applications of TCA were in the prediction of geophysical parameters, including soil moisture, wave height, and ocean wind speed (Dorigo et al., 2010, Crow & Van Den Berg 2010; Levizzani et al. 2020).

TCA was not widely employed in research to quantify the uncertainty in rainfall estimates. However, applicability has increased in recent years compared to earlier years, with particular progress in the use of Python statistical packages.

SREs could play a significant role in explaining the present state of fluctuating climate patterns (Dinku et al. 2018a, b). Also, the negative impacts of extremes of rainfall events on rain-fed food crops and risk managements (Murray and Ebi 2012). In addition, the hydro-meteorological multi-hazard early warning (Petropoulos and Islam 2017), agriculture and food security early warnings and actions. In Africa, specially Eastern Africa, the number of stations and networks has gradually decreased over time since the 1980s (Dinku et al. 2014; Funk et al. 2015a, b). In the recent years, SREs and gridded datasets have been used to assess the past and recent changes and variability in rainfall in the light of the decline in observation networks over Africa and other regions (Funk et al. 2015a, b; Nicholson & Klotter 2021).

Quantifying oversights and uncertainties surrounding SRE properties are crucial to ensuring their appropriate usage in a variety of socioeconomic sectors applications (Levizzani et al. 2020). The precipitation form, precipitation variety within the sensor footprint, and sensor frequencies and channels, and the method used to translate sensor retrieval data into precipitation rate are only a few of the variables that affect these products' accuracy and precision. The most frequent sources of inconsistency in SRE products are as follows: (1) sample uncertainty that are brought by the few satellite overpasses at a particular area on a given day (2) parameter used in calibration of uncertainty and errors, (3) retrieval processes and manner in which algorithm formulated (4) errors in pre-existing databases and catalogs (Stephens & Kummerow 2007; Levizzani et al. 2020).

Several studies by Dinku et al. in multiple areas in East Africa validated different SREs at different temporal and spatial scales (Dinku et al. 2011a, 2011b, 2014a, 2014b, 2018), by Maidment et al., (2013, 2014, 2017), other studies are (Hirpa et al., 2010, Romilly & Gebremichael 2011, Young et al., 2014, Diem et al., 2014, Worqlul et al., 2014, Awange et al. 2016) among others. Many of these validations, which have concentrated on East Africa sub-regions and the wide range of terrain, have revealed the difficulties of satellite rainfall retrieval over most parts of region. The primary finding of what has emerged from these several researches is that the accuracy of satellite rainfall estimates over the regions varies substantially depending on climate, terrain, and seasonal rainfall patterns. Therefore, assessing the quality of SRE, temporal and spatial climate information produced by climate services providers from such as National Meteorological and Hydrological Services (NMHSs) and Regional Climate Centers (RCCs) can advise and help policy makers to plan and strengthen the resilience of communities to withstand against extreme rainfall events

through reliable and timely climate information (Oloo and Omondi 2017).

The goal of this paper is to evaluate the performance of eight satellite-based products (CHIRPS v2.0, TAM-SAT v3.1, NOAA-CPC ARC2, NOAA-CPC RFEv2, PER-SIANN-CDR, CMORPH RT V0.x BLD, GPM -IMERG V06, TRMM 3B42 v7), CPC-unified gauge gridded, spatial interpolated of 65 rain gauges in east Africa. The main strength of this work, compared to previous studies of the region show that it uses a greater number of SREs and covers eight countries in east Africa, and uses 20 continuous statistical, categorical and volumetric indices for the first time in the region. Also, our validation based on 105 rain gauge in the region. The Study Area, the data, and validation techniques are covered in Sect. 2. Section 3 consists of the discussions and findings, while Sect. 4 offers a summary and conclusion.

2 Data and methods

2.1 Description of the study area

The Inter-Governmental Authority on Development (IGAD) region of eastern Africa consist of eight members' states

include Kenya, Ethiopia, Somalia, Sudan, Eritrea, South Sudan, Djibouti and Uganda which covers 5.2 million km². As shown in Fig. 1, the region has borders with Libya, Egypt, Central African, Chad, Congo, Tanzania and Rwanda with the locality possessing a population of approximately 230 million (Farah Hersi & Akinola 2024). The average population density estimated to be above 30 persons within one km². The characterized by high population growth rates, hence high risks of food insecurity. Additionally, (Omiti, 2013) noted that, the region retains varied ecosystems, agro-climatic, agro-ecological zones, diverse altitudes and highlands ranging from 150 m below sea level (Dallol) in Ethiopia to about 4600 m (Mount Kenya) in Kenya (<https://igad.int/about-us/the-igad-region>). The region is composed of seventy percent of Arid and Semi-Arid exposed to less than 600 mm annual precipitation. The remaining part of this region experiences a wide range of climates and landscapes, including tropical rainforests, swamp areas, and cool highlands.

2.2 Data

Data used are 105 rain gauge observations from eight (8) member states of Intergovernmental Authority on Development (IGAD). These data are obtained from IGAD Climate

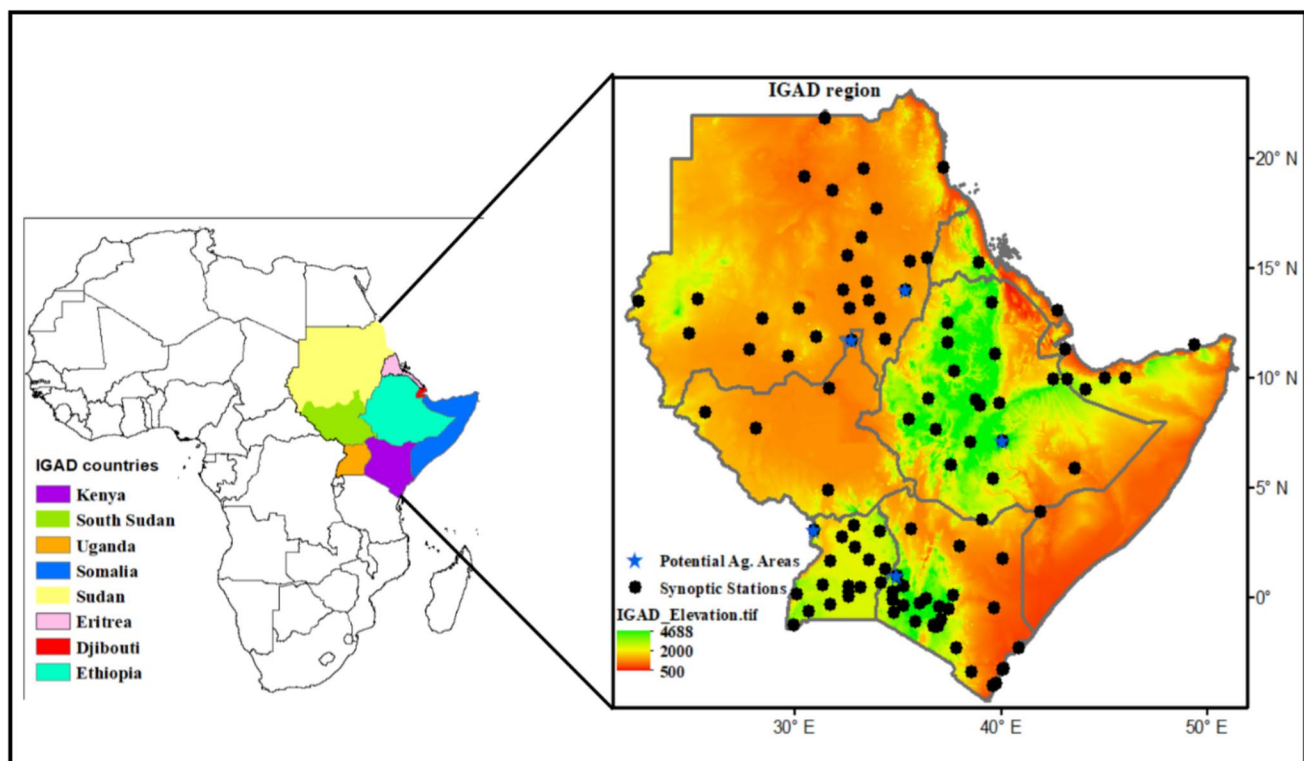


Fig. 1 Elevation map of the IGAD region of Eastern Africa showing the location of 105 rain gauge stations (*) and five potential agricultural areas (*) used to analyze the temporal and statistical metrics at sub-national level

Prediction and Application Centre (ICPAC) database. The 105-rain gauge from 1981–2022 used as reference datasets. The second type of datasets used are Nine (9) different Satellites-based Rainfall Estimates (SREs). The nine (9) SREs datasets to selected the best performed dataset to assess the observed rainfall extreme events in East Africa. The comprehensive and detailed key features, data generation methods, sources and processing techniques, applications, advantages, and limitations of each dataset are elucidated as follows:

- (a) Climate Hazards Group InfraRed Precipitation with Station data (CHIRPS).

The Climate Hazards Group InfraRed Precipitation with Station data (CHIRPS) is a high-resolution global precipitation dataset developed by the Climate Hazards Group at the University of California, Santa Barbara (Funk et al. 2015a, b). CHIRPS provides rainfall estimates derived from satellite data, blending it with ground-based station data (rain gauge). The dataset spans from 1981 to the present with a resolution of 0.05° on daily, temporal, and monthly timescales and covers all global land surfaces between 50°S and 50°N , making it valuable for monitoring droughts, floods, and climate trends, particularly in regions with sparse weather station networks, such as sub-Saharan Africa.

- (b) Tropical Applications of Meteorology using SATellite and ground-based observations (TAMSAT).

The Tropical Applications of Meteorology using SATellite and ground-based observations (TAMSAT) African Rainfall Climatology and Time Series (TARCAT) v3.1 is a dataset developed by TAMSAT at the University of Reading, specifically designed for monitoring rainfall over Africa (Maidment et al., 2014; Tarnavsky et al. 2014). TARCAT aims to provide accurate and timely rainfall estimates, with a focus on supporting applications in food security, hydrology, and disaster risk management, particularly in Africa. The key features of TARCAT v3.1 include a spatial resolution of 4 km (approximately 0.04°) and temporal coverage from 1983 to present, with a temporal resolution of daily, dekadal (10-day), and monthly. TARCAT v3.1 is based on satellite data (Meteosat thermal infrared observations) and calibrated using rain gauge data to improve accuracy.

- (c) NOAA Climate Prediction Center African Rainfall Climatology Version 2 (ARC2).

The NOAA Climate Prediction Center African Rainfall Climatology Version 2 (ARC2) is a satellite-based rainfall dataset specifically developed to monitor precipitation over Africa (Novella & Thiaw 2013). It was created by the NOAA Climate Prediction Center (CPC) and is widely used for

drought monitoring, agricultural planning, and hydrological studies across the African continent. The key features of ARC2 are temporal coverage from 1983 to present, spatial coverage for the entire African continent, spatial resolution of 0.1° (~ 10 km), and temporal resolution of daily. ARC2 primarily relies on geostationary satellite imagery from Meteosat thermal infrared (IR) sensors, which are merged with rain gauge data to improve the accuracy of rainfall estimates. ARC2 uses algorithms that combine satellite-based IR observations with rain gauge data from the Global Telecommunication System (GTS). This method enhances the spatial resolution and makes rainfall estimates more accurate in areas with sparse station data.

- (d) Climate Prediction Center (CPC) Unified Gauge-Based Analysis (CPC Unified V6).

The Climate Prediction Center (CPC) Unified Gauge-Based Analysis of Global Daily Precipitation version 6, or CPC Unified V6 (Xie et al., 2007), is a precipitation dataset produced by NOAA's Climate Prediction Center. It provides daily precipitation information globally by merging gauge observations from multiple sources, making it valuable for weather and climate research, monitoring, and prediction. Key features of CPC Unified V6 include global daily precipitation data at a high spatial resolution of $0.5^\circ \times 0.5^\circ$ (~ 50 km), spanning from 1979 to the present. This extensive coverage allows for detailed climate and precipitation analysis, particularly in regions with limited ground observation networks. The CPC Unified V6 integrates data from sources like the Global Telecommunication System (GTS), the Global Historical Climatology Network (GHCN), and regional climate centers. It includes improved quality control, enhanced data coverage, and better alignment with satellite-based precipitation estimates, increasing accuracy. While robust, CPC Unified V6 data relies on gauge-based observations, which may have spatial gaps in areas with limited weather station density, especially in remote or under-resourced regions.

- (e) African Rainfall Estimation Algorithm version 2 (RFE2).

The African Rainfall Estimation Algorithm version 2 (RFE2) is a precipitation estimation tool developed by the NOAA Climate Prediction Center (CPC) to provide near-real-time rainfall data over Africa (Herman et al. 1997). RFE2 combines satellite data from thermal infrared (IR) and microwave sensors with available gauge data. The RFE2 data sources include the Meteosat satellite for IR imagery and microwave observations from various satellite sensors with a spatial resolution of $0.1^\circ \times 0.1^\circ$ (~ 10 km), at daily temporal resolution from 2001 to the present, which makes

these datasets suitable for monitoring local-scale rainfall patterns over Africa. One limitation of RFE2 is the accuracy of satellite-rainfall-based estimates in regions with frequent cloud cover or during periods with sparse gauge data.

(f) Precipitation Estimation from Remotely Sensed Information using Artificial Neural Networks (PERSIANN).

PERSIANN-CDR (Precipitation Estimation from Remotely Sensed Information using Artificial Neural Networks—Climate Data Record) is a high-resolution global precipitation dataset developed to provide reliable, long-term rainfall estimates for climate studies and applications. Produced by the Center for Hydrometeorology and Remote Sensing (CHRS) at the University of California, Irvine, this dataset spans from 1983 to the present and is maintained for climate monitoring, trend analysis, and hydrological modeling. PERSIANN-CDR offers daily precipitation data at a $0.25^\circ \times 0.25^\circ$ spatial resolution (~25 km), suitable for both regional and global studies (Sorooshian et al. 2000). It uses an artificial neural network to process infrared (IR) satellite data for estimating rainfall. The dataset has been calibrated with the Global Precipitation Climatology Project (GPCP) monthly product, which helps maintain accuracy over time by correcting biases in the IR-based estimates. PERSIANN-CDR's long record and global reach offer significant benefits for historical climate studies and trend analysis, especially in data-sparse regions. As an IR-based product, PERSIANN-CDR can have limitations in accuracy under certain conditions, such as in regions with complex topography or during periods of low rainfall. IR data may sometimes overestimate or underestimate rainfall intensity, particularly compared to microwave-based or gauge-based estimates.

(g) NOAA-CPC morphing technique (CMORPH).

CMORPH RT V0.x BLD is part of the CMORPH (CPC MORPHing Technique) suite, designed to provide near-real-time precipitation estimates. Created by NOAA's Climate Prediction Center, this dataset uses satellite data to offer short-latency global precipitation estimates critical for weather monitoring and forecasting. CMORPH RT V0.x BLD serves various applications, especially in regions with limited access to timely ground-based precipitation data. CMORPH RT (Real-Time) delivers global precipitation estimates with a very short delay, making it valuable for applications needing near-instantaneous data, such as weather forecasting and emergency response. CMORPH RT updates every 30 min to 3 h, with a resolution of $0.25^\circ \times 0.25^\circ$ (~25 km) (Joyce et al. 2004). This product combines infrared (IR) and passive microwave (PMW) satellite data. Microwave data from polar-orbiting satellites provides direct precipitation estimates, while IR data from geostationary

satellites fills gaps and offers higher temporal coverage. The “morphing” technique adjusts rainfall estimates based on cloud movements observed in IR imagery, allowing the model to estimate rainfall even between satellite overpasses. The near-real-time capability and high temporal resolution provide actionable data for time-sensitive applications. However, because CMORPH RT relies heavily on IR data, it may be less accurate than gauge-calibrated products in estimating light rainfall or precipitation over complex terrains. IR data tends to estimate rainfall indirectly and can have limitations in accuracy compared to ground observations.

(h) Global Precipitation Measurement (GPM)—Integrated Multi-satellite Retrievals for GPM (IMERG).

The Global Precipitation Measurement (GPM)—Integrated Multi-satellite Retrievals for GPM (IMERG) Version 06 is a high-resolution precipitation dataset produced by NASA and the Japan Aerospace Exploration Agency (JAXA). IMERG V06 is part of the GPM mission, which provides global precipitation data by integrating information from a network of international satellites. IMERG V06 offers valuable precipitation estimates with high spatial and temporal resolution, making it widely used for climate monitoring, hydrological modeling, and disaster response. It provides global precipitation data at $0.1^\circ \times 0.1^\circ$ (~10 km) spatial resolution, available at half-hourly, hourly, and daily intervals, covering latitudes between 60°N and 60°S . IMERG integrates data from multiple satellite sensors, particularly from the GPM Core Observatory's Dual-Frequency Precipitation Radar (DPR) and GPM Microwave Imager (GMI), as well as data from other polar-orbiting satellites with passive microwave sensors (Hou et al. 2008). It combines microwave and infrared data using advanced algorithms to produce accurate precipitation estimates, with microwave data offering better rainfall measurement and infrared data providing higher temporal frequency. IMERG V06 is valuable for studying trends in precipitation, seasonal variations, and the impact of climate change on rainfall distribution. Its high resolution and frequent updates make it ideal for both research and real-time applications. The integration of various satellite sources helps improve the accuracy and reliability of precipitation estimates. IMERG V06 may have limitations in areas with frequent snowfall or mixed precipitation, as the accuracy of satellite-based estimates can be lower for non-liquid precipitation.

(i) Tropical Rainfall Measuring Mission (TRMM).

The Tropical Rainfall Measuring Mission (TRMM) 3B42 Version 7 (3B42 v7) is a widely used global precipitation dataset developed by NASA and JAXA. It provides high-resolution precipitation data derived from TRMM satellite data

and other satellite sources, essential for climate research, hydrological modeling, and weather monitoring in tropical and subtropical regions. TRMM 3B42 v7 covers data between 50°N and 50°S, focusing on these regions, with a $0.25^\circ \times 0.25^\circ$ spatial resolution (~25 km) (Huffman et al. 2007). It offers three-hourly precipitation estimates and daily accumulated data from 1998 to 2019. The 3B42 v7 algorithm integrates data from TRMM's Microwave Imager (TMI) and Precipitation Radar (PR), along with additional passive microwave observations from other satellites. Infrared (IR) data from geostationary satellites enhance temporal resolution, while ground-based rain gauges improve accuracy through monthly calibration. TRMM 3B42 v7 is used to analyze precipitation patterns, seasonal rainfall variability, and trends in extreme weather events. A limitation is that it does not cover areas beyond 50° latitude, restricting its use for global studies requiring data at higher latitudes. As TRMM has been succeeded by the GPM mission, 3B42 v7 is no longer updated beyond 2019, so users now rely on GPM-IMERG for recent precipitation data.

The summary of inputs such as gauge, model re-analysis, radar, Thermal Infrared (TIR), Near Infrared (NIR), Passive Microwave (PMW), Visible (VIS)) summarized in Table 1. Due to variation in resolution and temporal time scale, all these datasets were rescaled to 5 km (0.05 deg), and datasets from 2001 to 2020 were selected for analysis to facilitate comparison and validation.

2.3 Methods

2.3.1 Rain gauge quality check

The study conducted three quality control checks on 105 rain gauge stations. The first check involved verifying the gauge coordinates, and the results were displayed on the OpenStreetMap tool for verification and correction of the actual coordinates. The second check focused on identifying

outliers in the rain gauge values using a neighborhood selection approach. The outlier parameters used included a minimum of 4 neighboring stations, a maximum of 15 neighboring stations within a maximum search distance of 120 km radius, and an elevation difference of 800 m, as recommended by the Climate Data Tool developers (Dinku et al. 2022). Lastly, the study performed a homogeneity test using the Pettitt Test (Xie et al. 2014). The test parameters used were a maximum of 15 breaks, a minimum segment length of 24, a minimum data span of 5 years, a minimum non-missing fraction (available data) of 0.5, and a confidence level of 95% (Dinku et al. 2022).

2.3.2 Bilinear interpolation method

The 9 SREs are in different resolutions, therefore we adopted the bilinear interpolation approach used by researchers Song and Yan (2022) to solve the difficulties caused by the disparities in SRE resolutions. All SRE dataset were rescaled to ten-kilometer (0.1 deg) resolutions. This was done to facilitate the spatial comparison. Bilinear interpolation calculates the value scaled low/high resolution at an intermediate point within a grid cell based on the values at the four surrounding grid points. The process involves two linear interpolations in one direction (usually the x-direction) followed by a linear interpolation in the perpendicular direction (y-direction). The 105 rain gauge observations were interpolated spatially using the Modified Shepard interpolation method at the dekadial timescale, then point data extracted from all 9 SREs based on the coordinates (latitudes and longitudes) of 105 synoptic stations. This was done to facilitate comparison with the raw data of the 105 rain gauge observations.

Table 1 The Satellite Rainfall Estimates (SREs) that will be used in this study

Data	Inputs	Spatial Resolution	Period Used	References
CHIRPS v2.0	CHPCLIM, TIR, TRMM 3B42, CFSv2, gauges	0.05°	1981–2020	Funk et al. (2015a, b)
TAMSAT v3.1	TIR	0.0375°	1983–2020	Maidment et al. (2014)
NOAA-CPC ARC2	IR, gauges	0.1°	1983–2020	Novella and Thiaw (2013)
CPC unlimited version 6	Gauges gridded	0.5°	1979–2020	Xie et al., (2007)
NOAA-CPC RFEv2	TIR, PMW, gauge	0.1°	2001–2020	Herman et al. (1997)
PERSIANN-CDR	TIR, PMW	0.25°	1983–2020	Sorooshian et al. 2000
CMORPH RT V0.x BLD	TIR, PMW	0.07°	2000–2020	Joyce et al. (2004)
GPM -IMERG V06	TIR, PMW, gauge	0.1°	2001–2020	Hou et al. 2008
TRMM 3B42 v7	TIR, VIS, PMW, radar, gauges	0.25°	1998–2015	Huffman et al. (2007)

2.3.3 Total rainfall climatology

The total rainfall climatology of 9 RSE (2001–2020) was computed using an arithmetic mean over a decadal (20-year period). This used as baseline for spatial comparison and detection in patterns of total rainfall of 20-year climatology period (2001–2020). In this case, the arithmetic mean is the sum of total rainfall divided by the number of years included in the study. The spatial patterns of total rainfall for 9 RSEs computed using Eq. (1)

$$\bar{X} = \frac{1}{N} \sum_{i=1}^n X_i \quad (1)$$

Table 2 Descriptions of 20 statistical metrics, used in the validation of 9 SREs

	Name	Formulas	Perfect Score
Statistical metrics	COR	$CC_{GS} = \frac{\frac{1}{n} \sum_{i=1}^n (O_i - \bar{O})(S_i - \bar{S})}{\sqrt{\frac{1}{n} \sum_{i=1}^n (O_i - \bar{O})^2 \cdot \frac{1}{n} \sum_{i=1}^n (S_i - \bar{S})^2}}$	1
	PBIAS	$PBIAS(\%) = \frac{\sum_{i=1}^n (S_i - O_i)}{\sum_{i=1}^n O_i} 100\%$	0
	ME	$ME = \frac{1}{N} \sum (S - O)$	0
	MAE	$MAE = \frac{1}{N} \sum_{i=1}^n (S_i - O_i) $	0
	RMSE	$RMSE = \sqrt{\sum_{i=1}^n \frac{(S_i - O_i)^2}{n}}$	0
	NSE	$NSE = 1 - \frac{\sum_{i=1}^n (S_i - O_i)^2}{\sum_{i=1}^n (O_i - \bar{O})^2}$	1
	IOA	$IOA = 1 - \frac{\sum_{i=1}^n (O_i - S_i)^2}{\sum_{i=1}^n (S_i - O_i - O_i - O)^2}, 0 \leq d \leq 1$	1
	POD	$POD = \frac{A}{A+C}$	1
	POFD	$POFD = \frac{B}{B+D}$	0
	FAR	$FAR = \frac{B}{A+B}$	0
	CSI	$CSI = \frac{A}{A+B+C}$	1
	HSS	$HSS = \frac{2.(A.D-B.C)}{(A+C).(C+D)+(A+B).(B+D)}$	1
	MQB	$MQB = \sum_{i=1}^n \frac{(P_S P_S \geq t) - (P_O P_O \geq t)}{n}$	
	MQE	$MQE = \sum_{i=1}^n \frac{(P_S P_S \geq t) - (P_O P_O \geq t)}{n}$	0
	VHI	$VHI = \frac{\sum_{i=1}^n (S_i (S_{i=1} > t \& O_i > t))}{\sum_{i=1}^n (S_i (S_i > t)) + \sum_{i=1}^n (O_i (S_i \leq t \& O_i > t))}$	1
	QPOD	$QPOD = \frac{\sum_{i=1}^n I(P_S P_S \geq t) P_O \geq t}{\sum_{i=1}^n I(P_S P_S \geq t) P_O \geq t + \sum_{i=1}^n I(P_O P_S \geq t) P_O \geq t}$	1
	VFAR	$VFAR = \frac{\sum_{i=1}^n (S_i (S_{i=1} > t \& O_i > t))}{\sum_{i=1}^n (S_i (S_i > t \& O_i > t)) + \sum_{i=1}^n (S_i (S_i > t \& O_i > t)) + \sum_{i=1}^n (S_i (S_{i=1} > t \& O_i \leq t))}$	0
	QFAR	$QFAR = \frac{\sum_{i=1}^n \sum_{i=1}^n I(P_S P_S) \geq t P_O \geq t}{\sum_{i=1}^n \sum_{i=1}^n I(P_S P_S \geq t) P_O \geq t + \sum_{i=1}^n I(P_O P_S \geq t) P_O \geq t}$	0
	VMI	$VMI = \frac{\sum_{i=1}^n (O_i \leq (S_i \leq t \& O_i > t))}{\sum_{i=1}^n (S_i (S_i > t \& O_i > t)) + \sum_{i=1}^n (O_i \leq (S_i \leq t \& O_i > t))}$	0
	VCSI	$VCSI = \frac{\sum_{i=1}^n (S_i (S_{i=1} > t \& O_i > t))}{\sum_{i=1}^n (S_i (S_i > t \& O_i > t)) + \sum_{i=1}^n (S_i (S_i > t \& O_i > t))}$	1

where \bar{X} = average number of yearly total rainfall amounts, n is the number of years sample, which is 20 years in this study, X_i = the value of each season and yearly the total rainfall amounts being averaged. The Standardized Precipitation Index (SPI) is used to assess the patterns of extreme rainfall events in rain gauges, interpolated gauges, and 9 SREs.

2.3.4 Statistical metrics

The performance of 9 SREs was validated using 20 statistical metrics to measure the goodness of SREs computed over all 105-rain gauge, and extracted dataset from locations of 105 spatial interpolated gauge in the IGAD region. The full names of 20 metrics are described in a study by

Omaya et al., (2023), therefore we didn't described them again just to avoid level of overlap with prior publications. Furthermore, we employed scatter plots, the cumulative distribution function (CDF), and colored code patriation to compare 105 rain gauge data and 9 SREs. Validation was performed on a decadal (10 days) temporal scale across IGAD region of Eastern Africa for the reference periods 2001–2020 for 9 SREs. The Table 2, described the mathematical formulas of 20 metrics used validation.

3 Results and discussions

3.1 Rain gauge quality check

The quality of rain gauge observations depends on the accuracy and reliability of rainfall measurements, as well as the quality check techniques used. Several steps and statistical methods, such as the rain gauge stations coordinate check, False Zero Check, Outliers values, and homogenous, are applied to ensure the quality of the rain gauge used in this study. A quality check was conducted on 105 synoptic

stations datasets over the IGAD region, which revealed two stations (Boosaaso in Somalia and Assab in Eritrea) with inaccurate station coordinates. The meteorological offices of these two port cities are located on land, while the synoptic station coordinates indicate that they are inside the Indian Ocean. This is not possible (see Fig. 2). Incorrect or misplaced coordinates typically result in reduced accuracy of the station's spatial interpolation, blending, or merging with satellite rainfall estimates (SRE) to form satellite-based gauge datasets. Therefore, it is necessary to adjust the coordinates before validating or computing extreme rainfall events.

The second quality control check on climate datasets gathered using synoptic stations is the False Zero Check. A "False Zero Check" typically refers to identifying and correcting instances where data is incorrectly recorded as zero when it should have a different value. The third quality control check on rain gauges was the outlier's check on climate data. The outlier's examination of 105 gauges in East Africa using temporal and spatial checks reveals significant extreme rainfall values across all of the countries in the region that are deemed to be outliers, particularly extraordinary rainfall

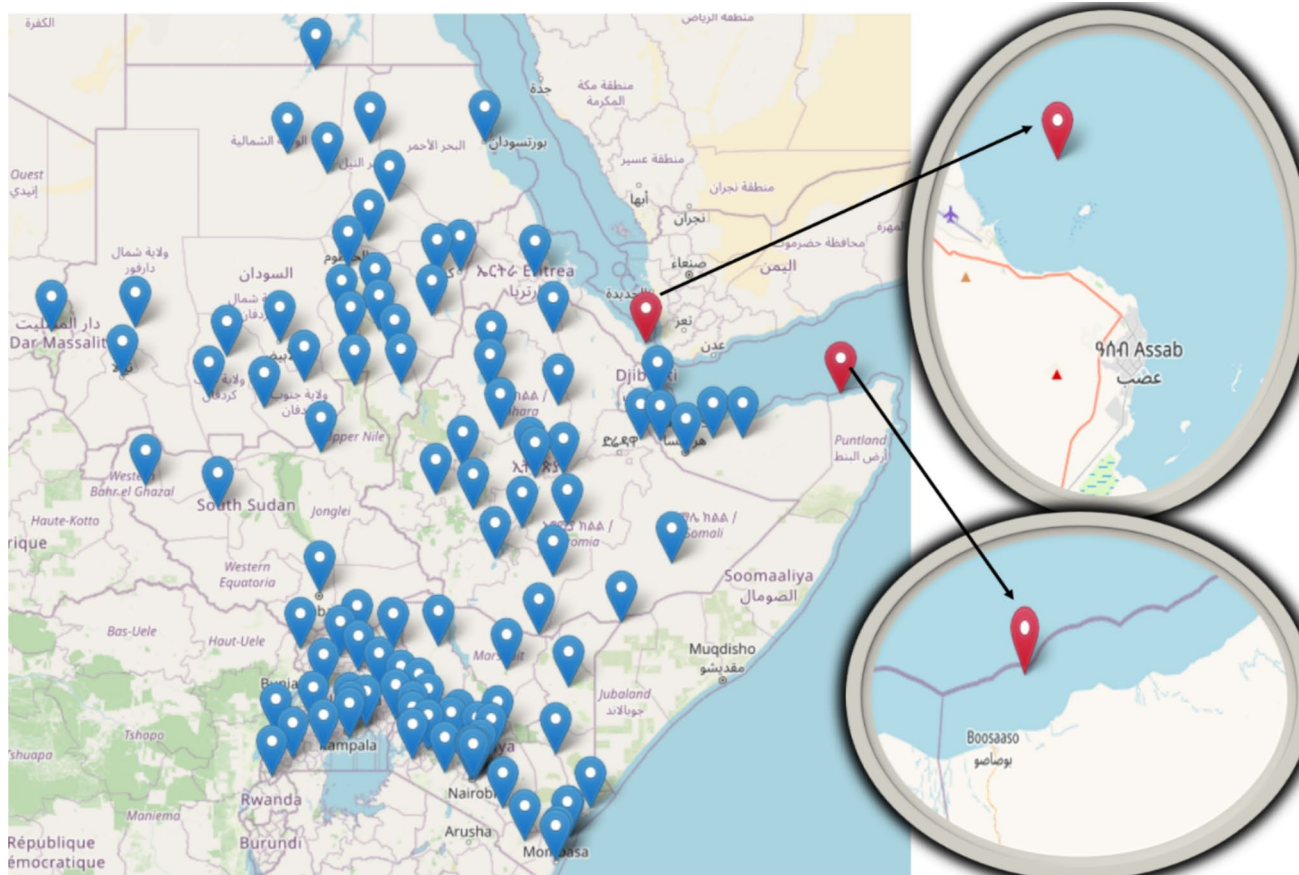


Fig. 2 Quality check on 105 rain gauge stations coordinates over the IGAD region

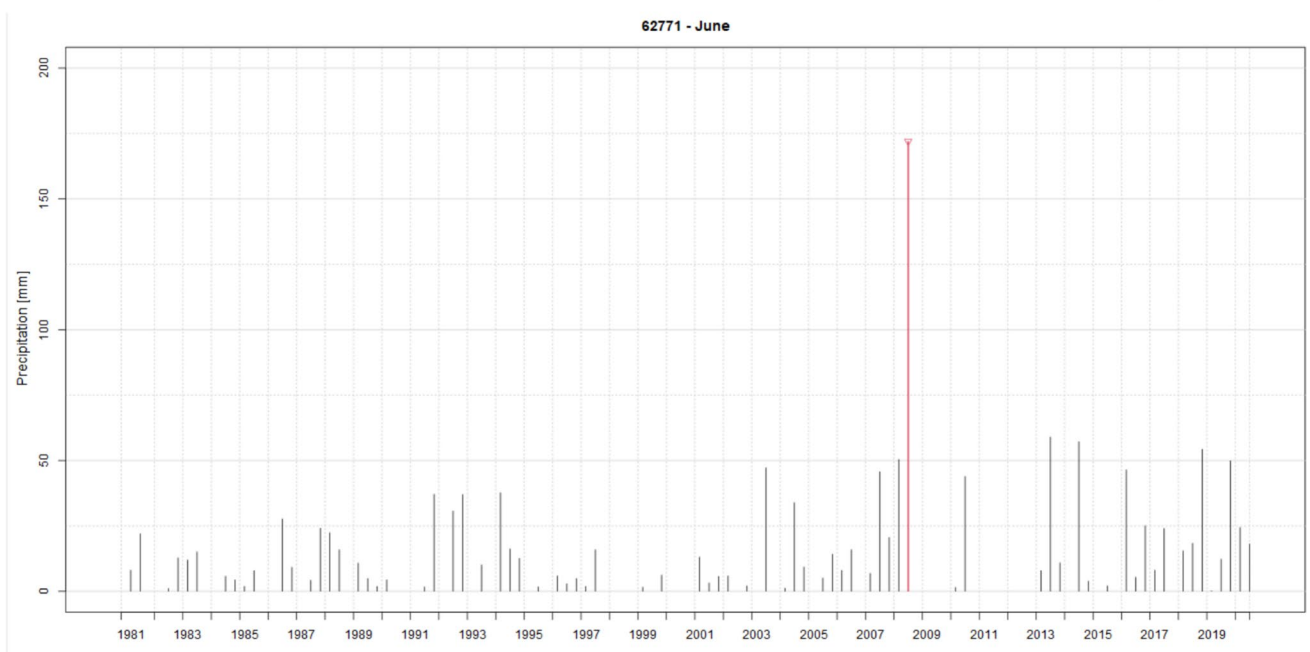
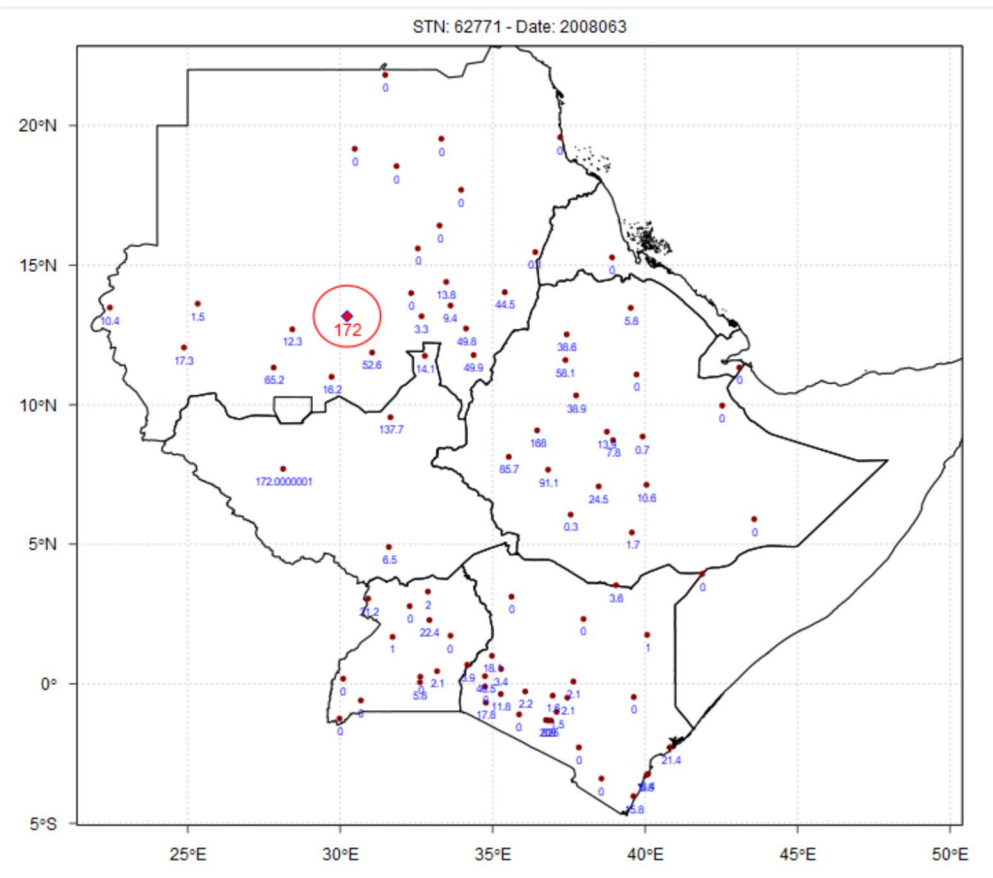


Fig. 3 Outliers check on 105 synoptic stations in IGAD region of eastern Africa

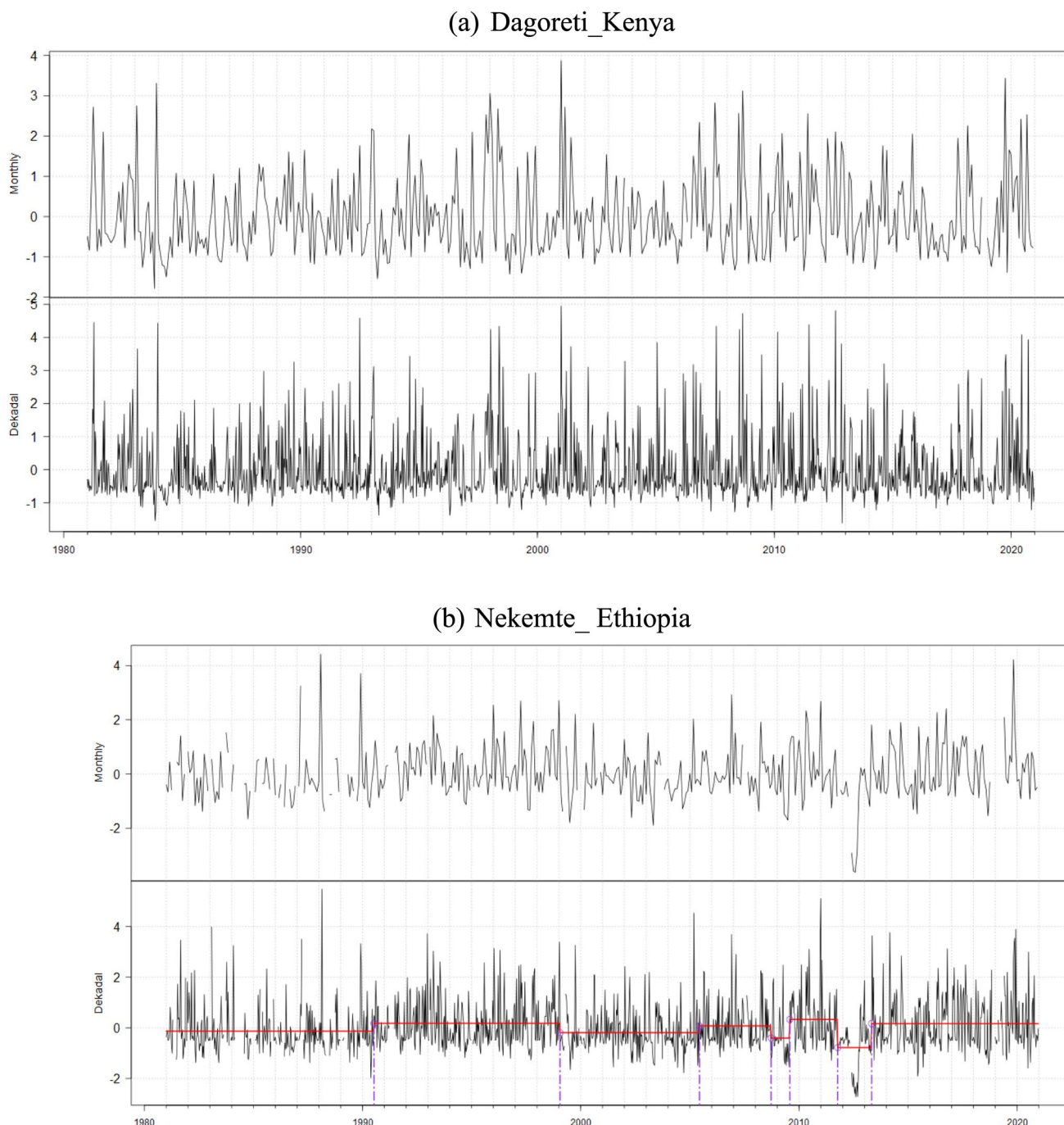


Fig. 4 Standard Normal Homogeneity Test (SNHT) for **a** Dagoretti in Kenya, **b** Nekemte in Ethiopia, **c** Kasese in Uganda

amounts (extreme values). The outlier test shows rainfall values that were true outliers, while others were incorrect outlier signals across all countries. One example is the EL-Obeid synoptic station in Sudan, which reported 172 mm of rainfall on the third dekad (21–30) of June 2008 (Fig. 3). This particular quantity of rainfall had never been recorded in the station's history, and as a result, it was regarded as an outlier rainfall value. But in fact, there is a real rainfall

amount recorded that day, which provides an explanation for the significance of checking for outliers when analyzing data on extreme rainfall values. Homogeneity is the fourth quality control on the rain gauge. It is used to find out if a climatic time series is consistent throughout time.

The Standard Normal Homogeneity Test (SNHT) (Alexandersson & Moberg 1997) is the third quality check used to test consistency in rain gauge measurements throughout

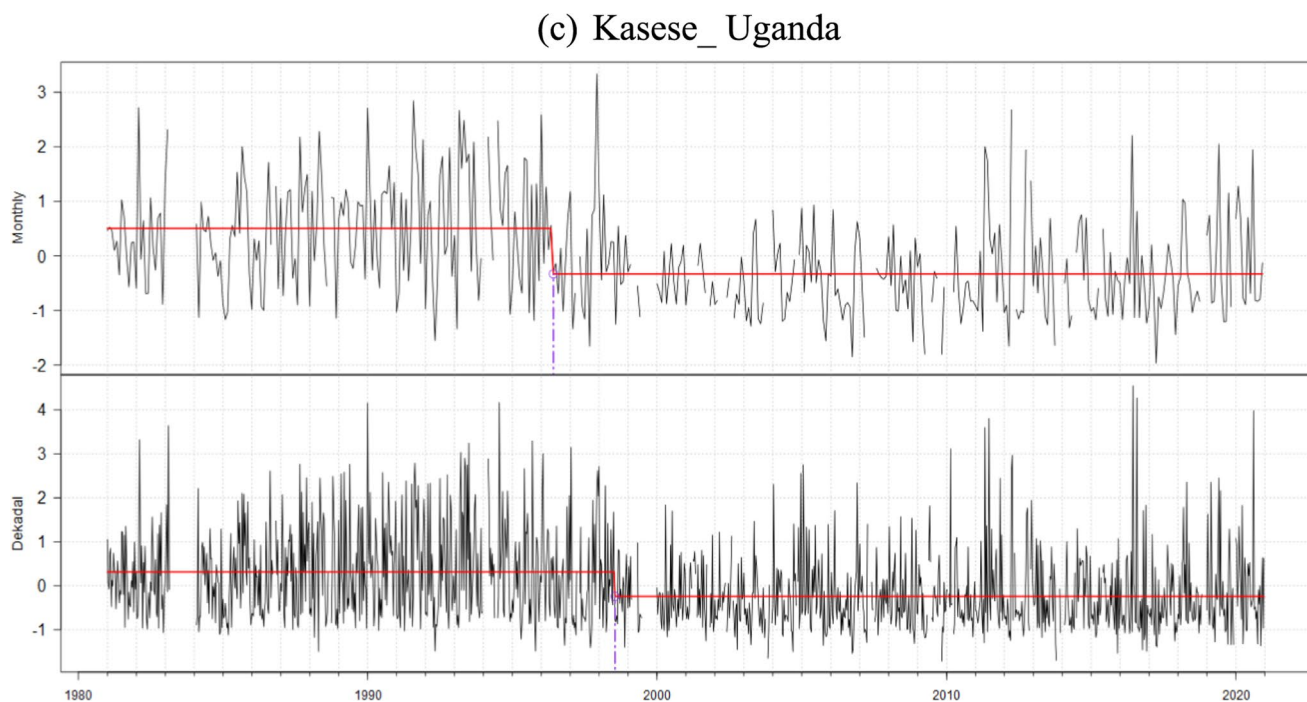


Fig. 4 (continued)

the years. The results of the SNHT are displayed in Fig. 4, illustrating significant differences in the quality of datasets between countries. The majority of synoptic stations in the IGAD region of eastern Africa have consistent time series (homogeneous), free from non-natural irregularities at the dekadal and monthly timescales. Most of these stations are located in main cities, urban areas, airports, or meteorological headquarters (Fig. 4a). Also, the quality check shows that some have more than two inconsistent time series, either due to high decadal variability, changes in daily rainfall intensities, digitization, or transmission of data (Fig. 4b). Considerable stations have high variation per few years, each decade (10 years) or more, either due to changes in station surroundings, relocation of stations, or changes in measuring instrumentation (Fig. 4c). In addition, there are gaps and missing data (3–7 years) due to insecurity and unrest in some parts of the region, reduced quality of synoptic stations, and increased inhomogeneity in time series. In some cases, where necessary, the outliers and inhomogeneity are corrected by going back to the original records at the country level, as recommended by Sylla (2018). In some cases, the amount of rainfall recorded by different SREs on the same day is used to confirm the possibility of the value being considered an outlier, while mean and quantile matching is used to adjust the inhomogeneity.

3.2 Total rainfall and annual cycle patterns

Figure 5 presents the spatial distribution of total rainfall patterns for 9 SREs and 105 gauges interpolated over the IGAD region during the MAM and JJAS seasons, using data averaged for the period of 2001–2020 (climatology). The results show major agreement in MAM and JJAS seasonal rainfall patterns of all 9 SREs and gauges interpolated over most parts of the region. Rainfall amounts of more than 400 mm are observed over Uganda, counties in Nyanza, highlands of western Kenya, and highlands of western Ethiopia, and are well represented by both the SREs and gauge interpolation. However, the CPC v6.0 under-estimated total rainfall over south-western Ethiopia. The results also indicate that the MAM and OND are very important seasons for Kenya, Uganda, and Somalia, while JJAS is crucial for South Sudan, Sudan, Ethiopia and Djibouti. Furthermore, well-represented rainfall patterns are observed over the Arid and semi-arid (ASAL) regions in Sudan, Djibouti, Eritrea and Kenya during MAM and JJAS. The gauge interpolation using the Modified Shepard interpolation method produces very good rainfall datasets and represents the regions where there were no synoptic stations (gauges). For countries such as Ethiopia, Kenya and Uganda Meteorological services, which have a considerable and well-distributed number of gauges, the Modified Shepard interpolation could be adopted for reliable

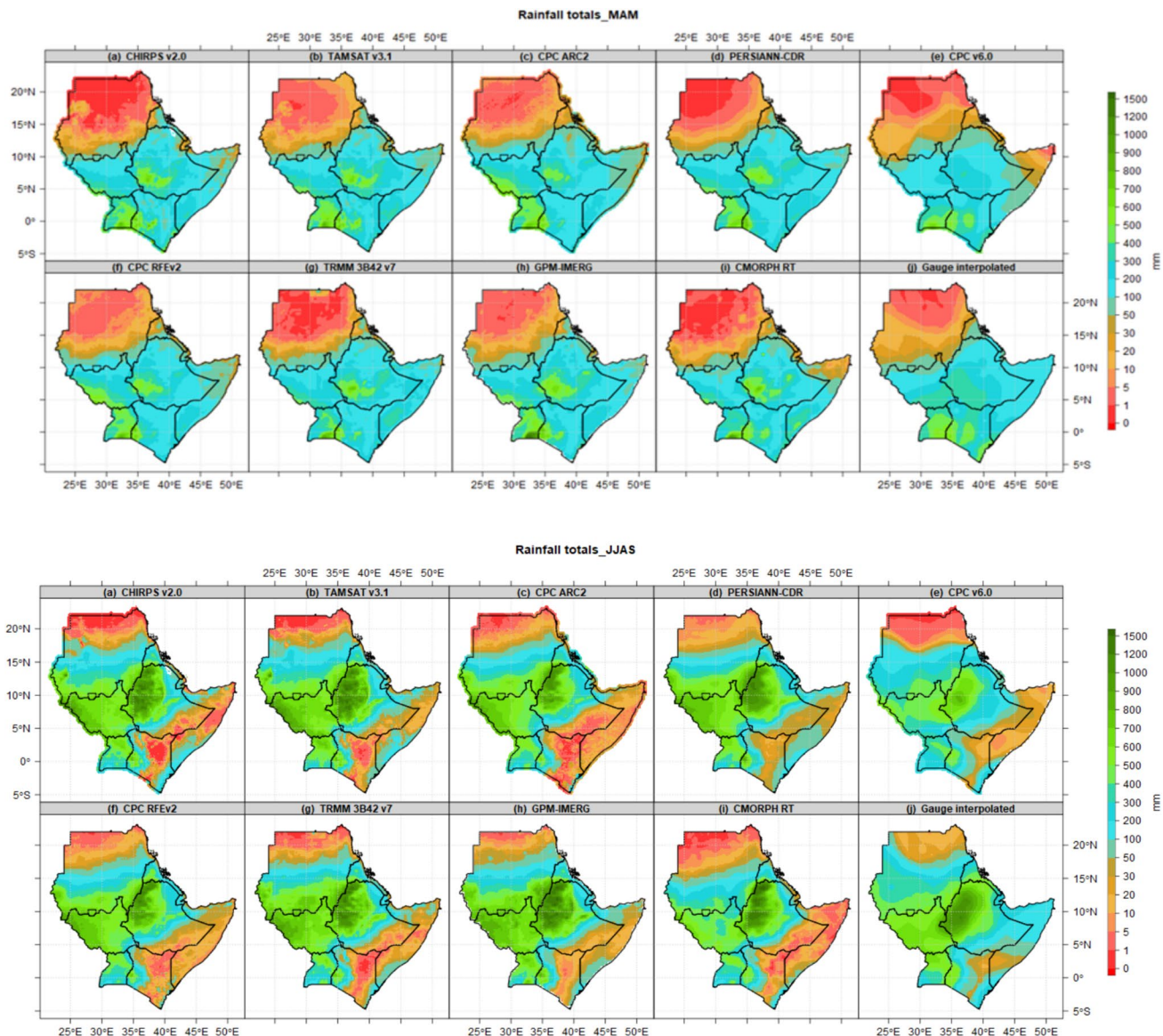


Fig. 5 Spatial distribution of total rainfall patterns for 9 SREs and 105 gauge interpolated during MAM and JJAS season

climate information services, rather than relying solely on the use of SREs.

Figure 6 shows the annual cycle over Al Qadaref in Sudan, El Renk in South Sudan, Robe in Ethiopia, Arua in Uganda and Kitale in Kenya. These five regions are considered as five food basket regions in the IGAD based on the quantities of food crops produced and agricultural opportunities. The results show all SREs and gauge capture rainfall picks, with unimodal rainfall regions observed over most parts of Sudan, Eritrea, Djibouti, South Sudan, western and northern Ethiopia, while bimodal rainfall is observed over Kenya, Uganda, Somalia and southern and central Ethiopia. The annual cycle confirms the importance of the MAM and OND seasons for the Equatorial

region and the JJAS season for the northern sector of the IGAD region. Most parts of the Lake Victoria basin in Uganda and Kenya received good rainfall from March to November, while the central and northern parts of South Sudan, Sudan and northern Ethiopia mainly receive rainfall from May to October. There is a peak of rainfall in April and August over the southern parts of Ethiopia and western Kenya. The annual cycle patterns show the possibility of successful agriculture and three cropping systems over Uganda and western Kenya.

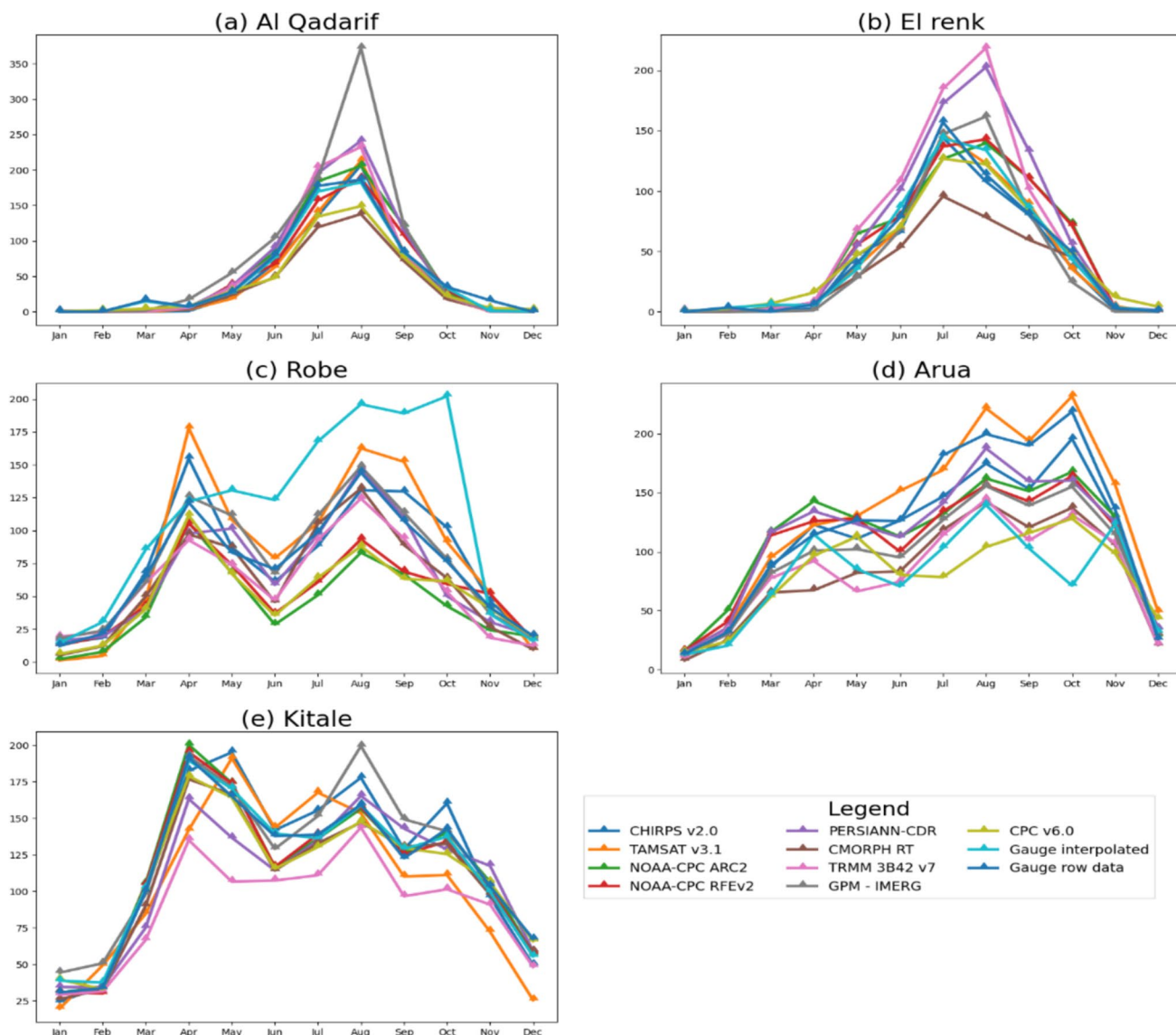


Fig. 6 Annual cycles patterns of 9SREs, gauge and interpolated gauge over five potential agricultural areas: **a** Al Qadarif in Sudan, **b** El renk in South Sudan, **c** Robe in Ethiopia, **d** Arua in Uganda and **e** Kitale in Kenya

3.3 Statistical metrics at regional level

The correlation coefficients (CC), Percent Bias (Pbias) and Root Mean Square (RMSE) between gauge observations, gauge interpolated, and nine (9) SREs at the dekadadal timestep are presented in Figs. 7, 8, and 9. The values are extracted at each 105-gauge, gauge interpolated and each 9 SREs coordinates. All nine SREs show high CC values of 0.8 to 0.9 over the northern parts of the Ethiopian highlands, most parts of Kenya and Uganda (Fig. 7). All nine SREs recorded low CC values of 0.1 to 0.4 over central and northern Sudan, northern Somalia and Djibouti. This is a clear indicator that the SREs are not performing well over desert and semi-arid areas compared to mountainous climates

(Dinku et al. 2011a). Gauge interpolated recorded almost one to one CC values (0.9–1) everywhere in the region. The JJAS season recorded low CC compared to the MAM and OND seasons. Most parts of Kenya and Uganda recorded the highest CC values due to the number of gauges used in blending with raw SREs datasets. The Rift Valley in Ethiopia appears to separate the higher CC values on the west and lower values on the eastern side. The CMORPH v1.0 CRT consistently performed better over Ethiopia and Kenya across the three seasons (Fig. 7j). It is important to note that differences in mountainous regions, synoptic systems and climatic zones played a significant role in the variation of low and high CC values. The low CC values over central and northern parts of Sudan could be interpreted as the impact of

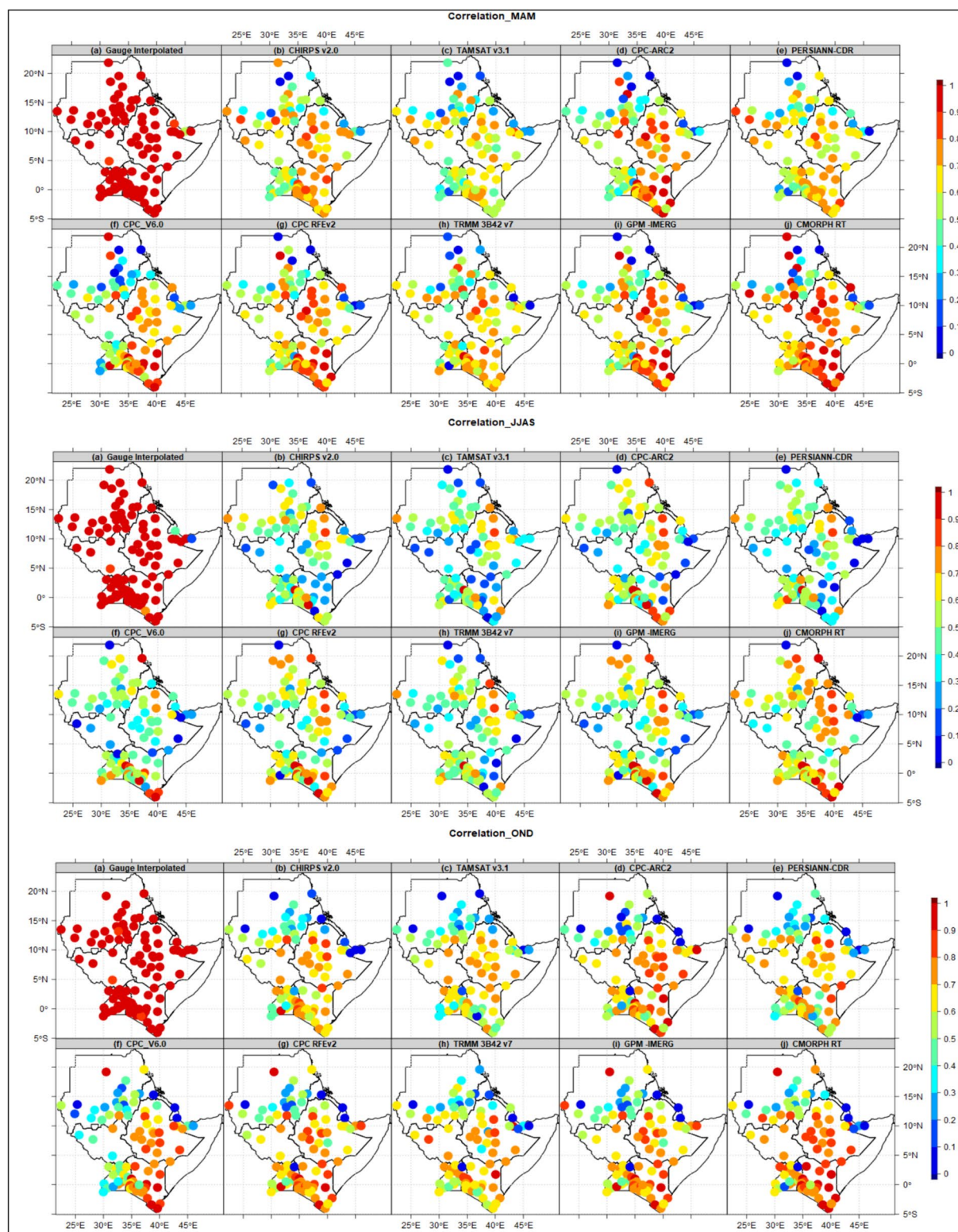


Fig. 7 The correlation coefficients (CC) of 9SREs, gauge and interpolated gauge. The values extracted at 105-gauge coordinates at the dekadal timestep

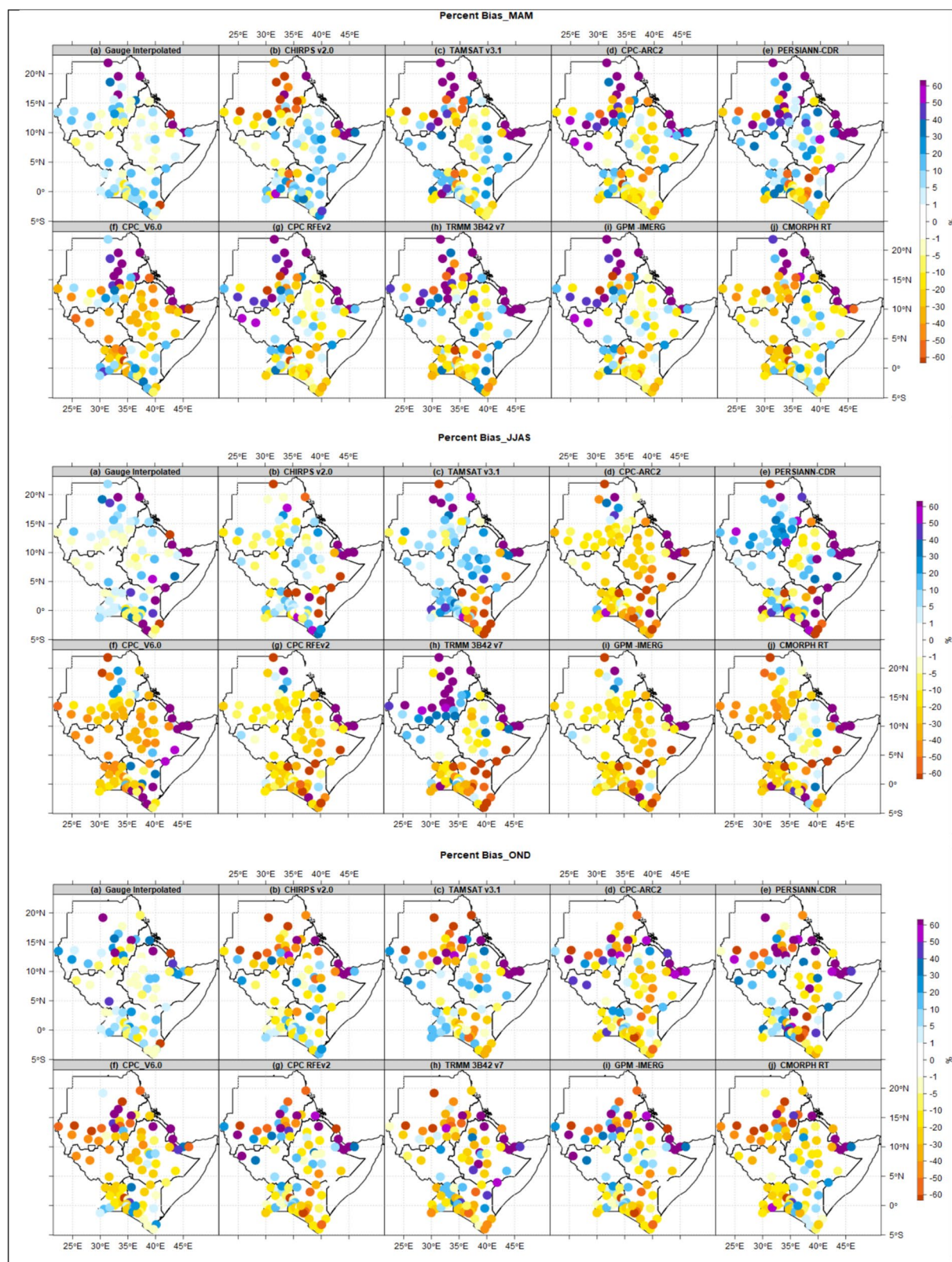


Fig. 8 Percent of Bias of 9SRE, gauge and interpolated gauge. The values extracted at 105-gauge coordinates at the dekadal timestep

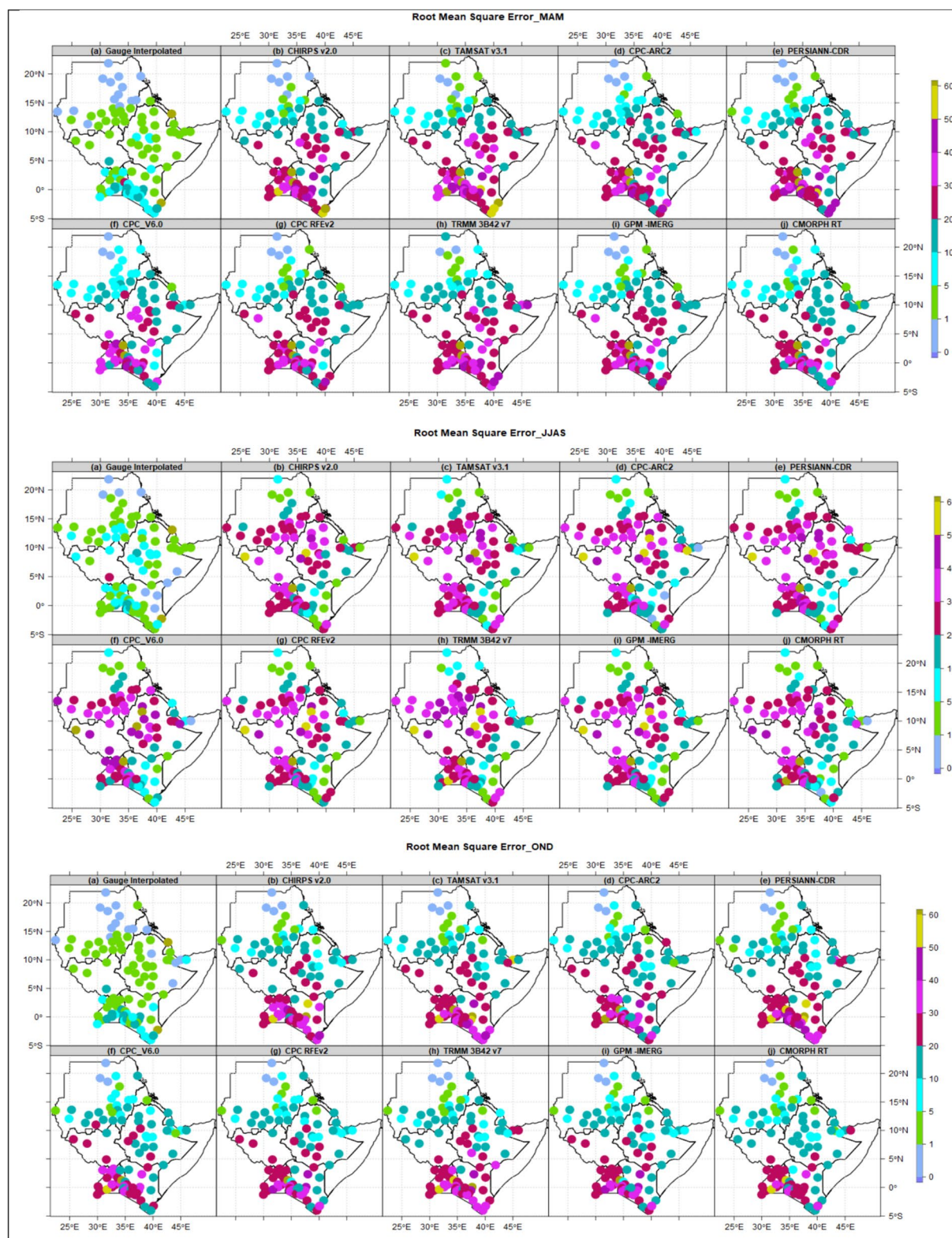


Fig. 9 Root Mean Square (RMSE) of 9SREs, gauge and interpolated gauge. The values extracted at 105-gauge coordinates at the dekadal timestep

a dry and warm desert climate. The coastal parts of Kenya observed higher CC values compared to the Sudan, Eritrea, Somalia and Djibouti coastal regions. This variation could be influenced by synoptic systems and orographic rainfall processes. These results are similar to the findings by Dinku et al. (2018a, b), where four SREs(CHIRPS, CHIRP, CPC ARC2, TAMSAT v3.1) were validated over eastern Africa.

Most parts of Sudan, Eritrea, Djibouti and the northern parts of South Sudan recorded the highest positive Pbias over-estimation of rainfall patterns), while the majority of SREs under-estimated rainfall over Kenya (negative Pbias) especially the southern parts of the country (Fig. 8). Across MAM, JJAS and OND seasons, over-estimation/under-estimation of rainfall was recorded in different parts of countries. This could be attributed to variation in climatic zones, climate systems influencing local climate within countries. CPC-ARC2, CPC v6.0, CPC-RFEv2, and GPM-IMERG were the most SREs that under-estimated rainfall patterns over most parts of the region, especially over Uganda during JJAS. This under-estimated rainfall could be attributed to different factors, such as cloud cover (thick or multiple layers of clouds) and the type of clouds, such as convective rainfall, which involves intense but localized thunderstorms (Ndiwa 2015). Uganda's diverse topography, including mountains, hills, and valleys, can affect precipitation distribution (Nsengiyumva 2019). Satellites may have difficulty accurately estimating rainfall in these complex terrains, where orographic effects lead to localized rainfall that might be missed or underestimated. The presence of large water bodies like Lake Victoria influences local climate and rainfall patterns (Ngoma et al. 2021). This finding aligns with the study by Awange et al. (2016), who found large negative biases in ARCV2, TRMM, CMORPH, TAMSAT, and GSMAp relative to GPCC over entire Africa especially the orographic regions of Ethiopia, Kenya, and Tanzania in East Africa. This is attributed to the fact that assimilated, gridded, and SREs have low skill in estimating the extremes of daily rainfall values (Ayehu et al. 2018). Additionally, the satellite-based quantitative precipitation estimation (QPE) products such as GPM-IMERG and Global Satellite Mapping of Precipitation (GSMAp) may not accurately capture the actual heavy precipitation due to a limitation in the use of infrared radiation (IR) to estimate precipitation: The movement of the clouds may not correspond with the movement and amount of the estimated precipitation (Tuttle et al., 2008; Chen et al. 2013; Zhu et al., 2022).

Due to the close relationship between CC and RMSE, the areas with the highest CC values recorded the lowest RMSE values (Fig. 9). The areas with the highest rainfall totals in the regions recorded highest RMSE, while ASAL in the region recorded the lowest RMSE. It seems that daily rainfall intensities, with over-estimated or under-estimated values increased the degree of error between gauges and

SREs. Sudan, Eritrea, Djibouti and northern Ethiopia recorded RMSE values of 6–10 during MAM and OND. Uganda, Kenya, South Sudan, southern Ethiopia, and central Ethiopia recorded the highest RMSE values (20–50) across three seasons (MAM, JJAS, and OND).

3.4 Statistical metrics at sub-national level

Figure 10 illustrates colored code portraits of 9 SREs with respect to gauge over Robe in Ethiopia during the MAM season, Al Qadaref in Sudan during JJAS season, and Kitale in Kenya during OND season. The evaluation was carried out utilizing 24 different statistical metrics. The findings indicate that concluding the best-performing SREs based on individual metrics, limited indices, and one rainfall season is premature. That is to say, it does not take into account the inclusion of SREs that perform well across a variety of index types, including continuous ones like bias, correlation, and RMSE, categorical ones like FAR and CSI, and volumetric ones like VHI, VFAR, VMI, and VCSI indices, or performance across specific locations. Individual SREs demonstrate skill variation across the 24 indices considered in the analysis. Some SREs scored exceptionally well on continuous indices but poorly on categorical and Volumetric indexes, and vice versa. Some SREs performed well in specific areas and seasons, while others performed poorly. According to the patterns over Robe, CMORPH RT showed the most best performing indexes, while CHIRPS v2.0 and TRMM 3B42 v7 performed well based on Volumetric indexes. The CPC v6.0 consistently performed well across majority of indexes. Based on continuous, Volumetric, categorical, and Volumetric indices, the patterns across Al Qadaref in Sudan for JJAS demonstrate that CMORPH RT, GPM L3 IMERG, and CPC ARC2 performed better. During OND, the CPC RFEv2 and CPC ARC2 are the best SREs performed across all indices for Kitale. Over the five potential agricultural areas examined in this study, and three seasons, the CMORPH RT outperformed other SREs on average. Similarly, the CMORPH emerged as the most suitable product using Three-Cornered-Hat (TCH) method and rain gauge-based validation methods (Awange et al. 2016). Validation using continuous indexes outperforms validation using categorical and Volumetric indexes in terms of quality, consistency, and representation.

Figure 11 shows scatter plots comparing the nine SRE products, rain gauge interpolated and gauge at dekadal time-scales. Kitale in Kenya, El Renk in South Sudan, and Arua in Uganda were selected as sampling locations for MAM, JJAS, and OND, respectively. There is substantial scattering for all 9 SREs products, particularly for rainfall quantities greater than 100 mm. During MAM season, the most spread out SREs over Kitale are CHIRPS v2.0, TAMSAT v3.1, PERSIANN-CDR, and TRMM 3B42 v7, while the

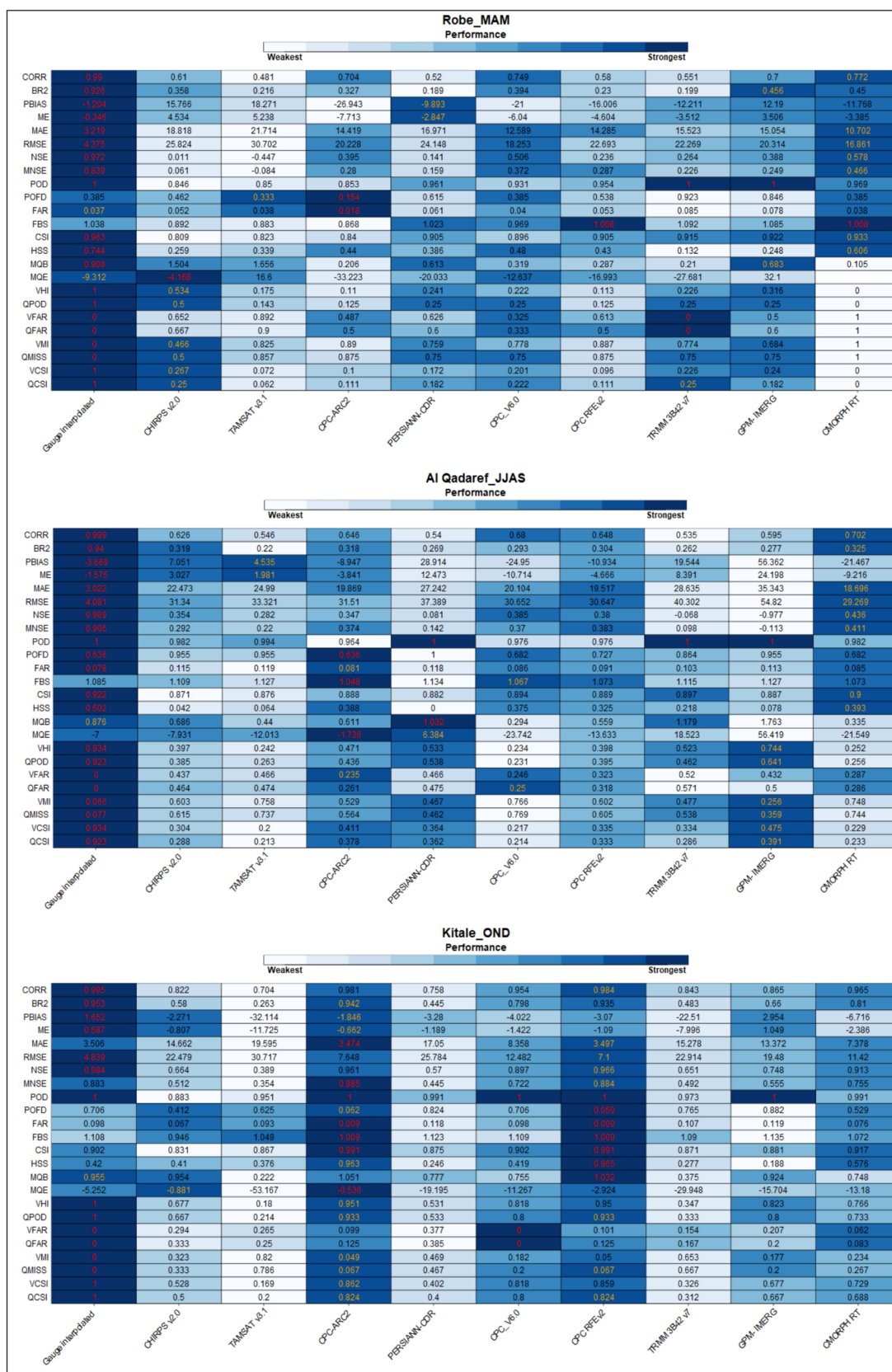


Fig. 10 Colored code portraits showing patterns of 24 different statistical metrics over Robe in Ethiopia during MAM season, Al qadaref in Sudan during JJAS season, and Kitale in Kenya during OND

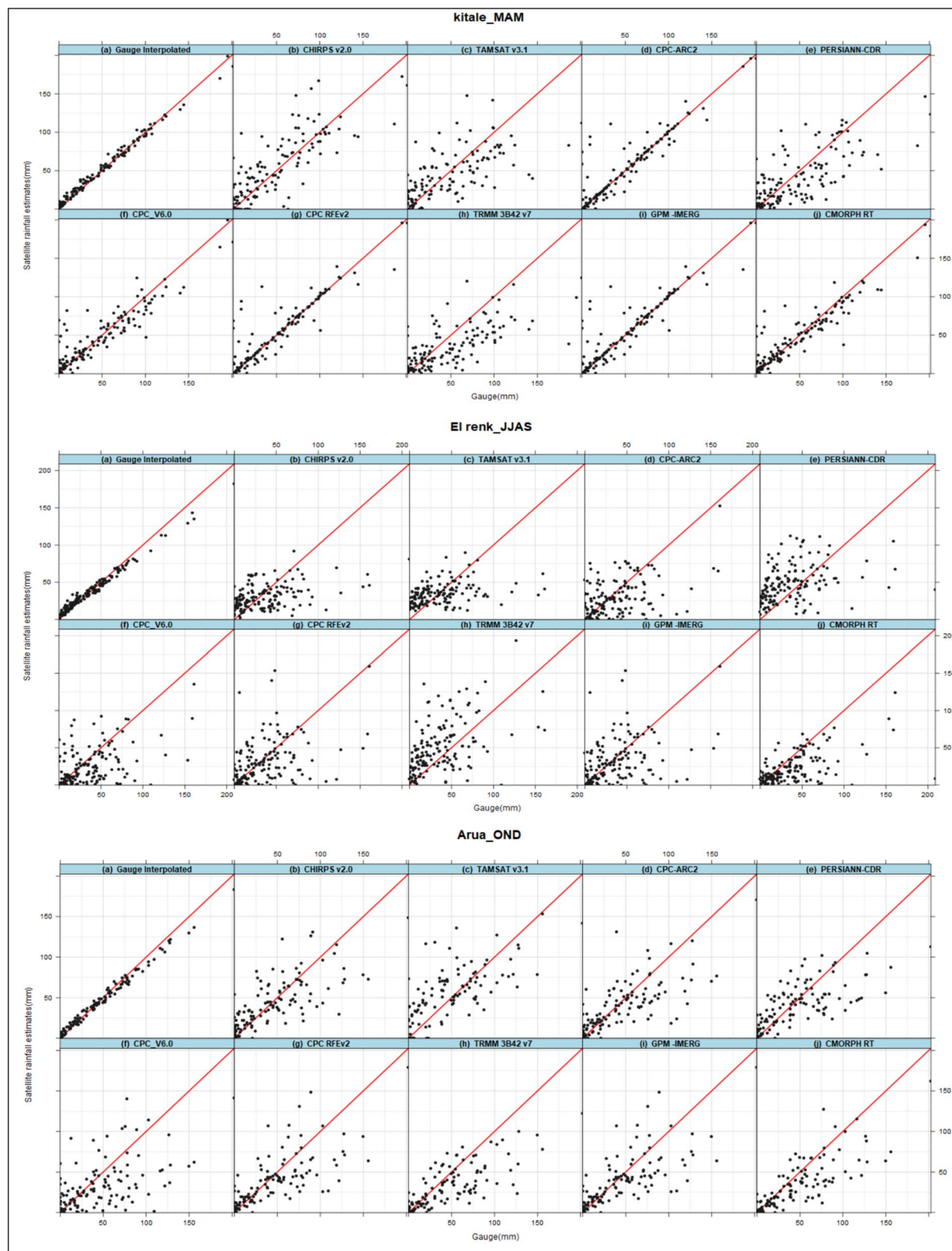


Fig. 11 Scatter plots comparing the 9SREs, gauge and gauge interpolated over Kitale in Kenya for MAM, El Renk in South Sudan for JJAS, and Arua in Uganda for OND at dekadial time-scales

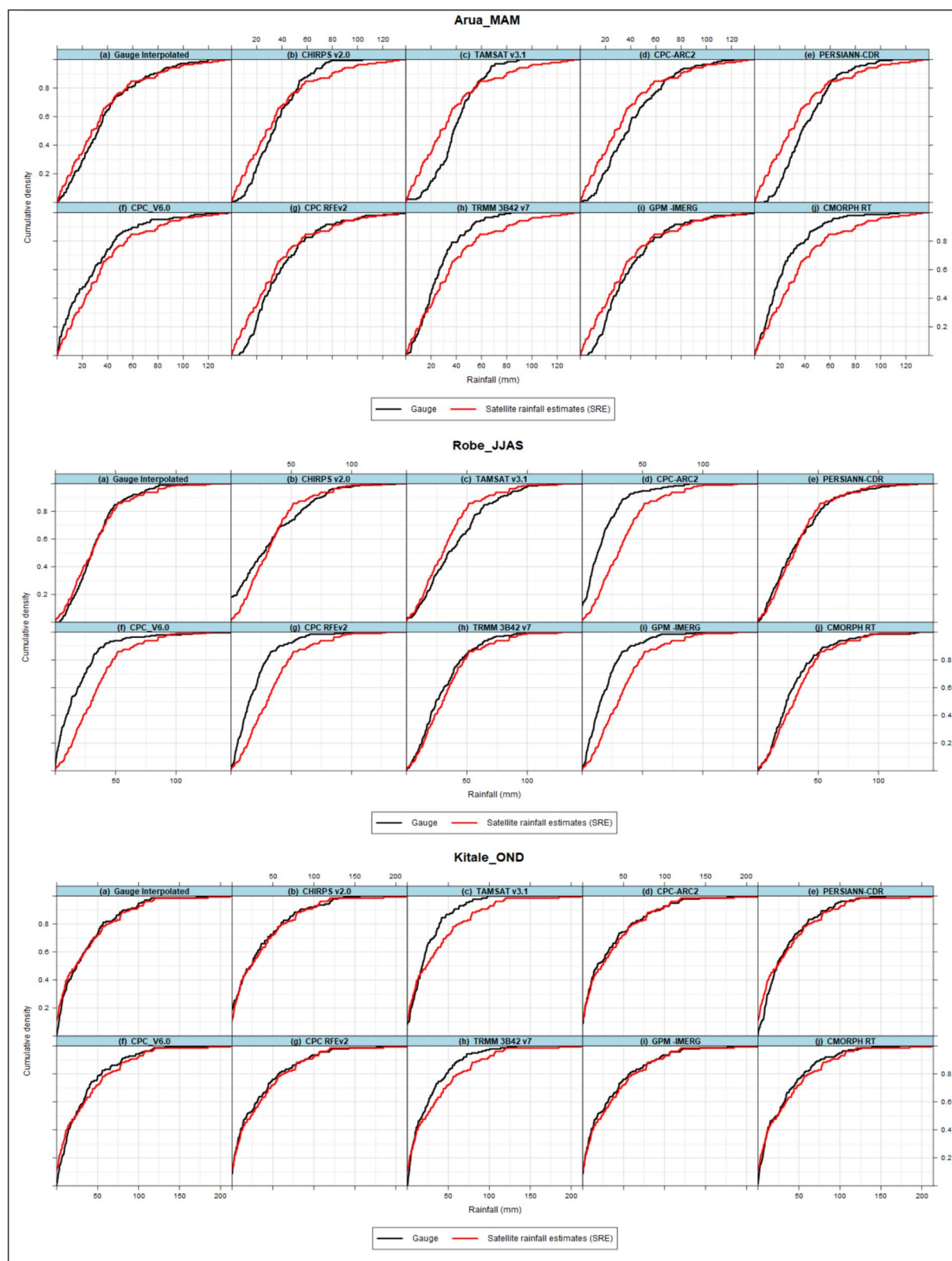


Fig. 12 Cumulative Distribution Function comparing the 9SREs, gauge and gauge interpolated during the MAM and JJAS season

least scattered are CMORPH RT, CPC ARC2, CPC RFEv2, and GPM L3 IMERG. As mentioned in the previous subsection, SREs performed poorly during the JJAS season, hence all 9 SREs are spread out in El renk as a sign of poor performance during the JJAS. The SREs that over-estimated rainfall patterns the most are PERSIANN-CDR and TRMM 3B42 v7, whereas the SREs that under-estimated rainfall totals the most are CHIRPS v2.0 and CMORPH RT. Again, the patterns over Arua during the OND season reveal that the majority of the 9 SREs recorded high scattered values, notably those greater than 100 mm. The CPC v6.0 and GPM L3 IMERG under-estimated rainfall the most, whereas TAMSAT v3.1 over-estimated rainfall. The variation in the results of statistical metrics, colored code portraits and scatter plots shows it is quite inclusive to identify and select the highest performing SREs based on a single season, a few indexes, or even one method, such as scatter plots.

The Cumulative Distribution Function (CDF) comparing each of the nine SREs throughout the MAM and JJAS seasons, gauge interpolated, versus gauge as a reference dataset, is shown in Fig. 12. The patterns for Arua, Robe, and Kitale respectively represent the MAM, JJAS, and OND seasons in Uganda, Ethiopia, and Kenya. The findings demonstrate that the performance of CDF's SREs varies depending on the SREs, area, and categories of rainfall (0–10, 10–50, 50–100, and 100–150 mm). According to the patterns over Arua, the TRMM 3B42 v7, CPC v6.0, and CMORPH RT underestimated rainfall, but the CHIRPS v2.0, TAMSAT v3.1, CPC ARC2, and PERSIANN-CDR overestimated rainfall below 80 mm and overestimated quantity beyond 80 mm. TRMM 3B42 v7, PERSIANN-CDR, and CMORPH RT are the best performing SREs, whereas CPC ARC2, CPC v6.0, and GPM L3 IMERG perform poorly over Robe during JJAS.

The spatial patterns of 9 SREs, statistical metrics at regional and sub-national levels show that the performance of satellite rainfall estimates over highlands compared to arid and semi-arid lands (ASALs) in the IGAD region varies significantly due to several factors, including topography, vegetation cover, and atmospheric conditions. The performance of satellite rainfall estimates also varies significantly between highlands and ASALs in East Africa. While ASALs may present fewer challenges due to simpler terrain and less vegetation, the complex topography and dense vegetation of highlands can lead to greater inaccuracies. However, our analysis shows that the performance of SREs over mountainous regions of the IGAD region is more accurate and reliable due to a higher density of rain gauge observations used in validation and inputs over the highlands of western Kenya, Ethiopia, and Uganda compared to lowland areas.

Also, the findings from validation and different statistical metrics used in this study show that SREs products provide valuable data for meteorological and socio-economic applications in the IGAD region, but several sources of

uncertainty can affect their accuracy. The first source of uncertainty in SREs is sensors, which often have coarse spatial resolution, making it difficult to capture small-scale rainfall events. The frequency of satellite overpasses can limit the ability to capture short-duration rainfall events. Sensor calibration errors and sensor drift over time can introduce biases in rainfall estimates (Maggioni et al. 2022). The second source of uncertainty is retrieval algorithms. Different algorithms make various assumptions about cloud properties, precipitation processes, and surface characteristics, which can introduce errors. Many algorithms rely on empirical relationships between observed satellite data (e.g., cloud top temperature) and rainfall, which may not be universally applicable. The complexity of algorithms can lead to different sensitivities to various atmospheric and surface conditions. The third is uncertainty due to variations in cloud structure and microphysics can lead to differences in how rainfall is estimated from satellite data (Kumar et al. 2020). Distinguishing between different types of precipitation (e.g., convective vs. stratiform) can be challenging and affect the accuracy of estimates. The fourth source could be from surface and environmental conditions such as land, ocean, snow-covered areas, which can affect the satellite's ability to detect and estimate rainfall accurately. Complex topography can influence the distribution and intensity of rainfall, leading to uncertainties in estimates (Dinku et al. 2011b, a). In addition, variations in atmospheric conditions (e.g., humidity, temperature profiles) can impact the accuracy of rainfall retrievals. The fifth source of uncertainty is the limited availability and quality of ground-based rainfall measurements can make it difficult to validate and calibrate satellite estimates (Suri & Azad 2024). Differences in the spatial and temporal resolution between satellite and ground-based measurements can introduce uncertainties in validation efforts. The sixth source of uncertainty is interpolating data from different satellite sensors and platforms that can introduce errors. Combining data from multiple sources (e.g., different satellites, radar, and ground-based measurements) involves assumptions and processing steps that can introduce uncertainties (Chen et al. 2020). The seventh source of uncertainty is seasonal variations in weather patterns and cloud properties that can affect the accuracy of satellite rainfall estimates (Kumah et al. 2022). The long-term changes in climate can impact the performance of algorithms developed based on historical data.

3.5 Extreme rainfall events

Figure 13 presents the standardized Precipitation Index (SPI), which shows the inter-annual variability and degree of agreement between the gauge, interpolated gauge, and 9 SRE in simulating the patterns of extreme rainfall events in terms of drought and flood patterns over Kitale in Sudan,

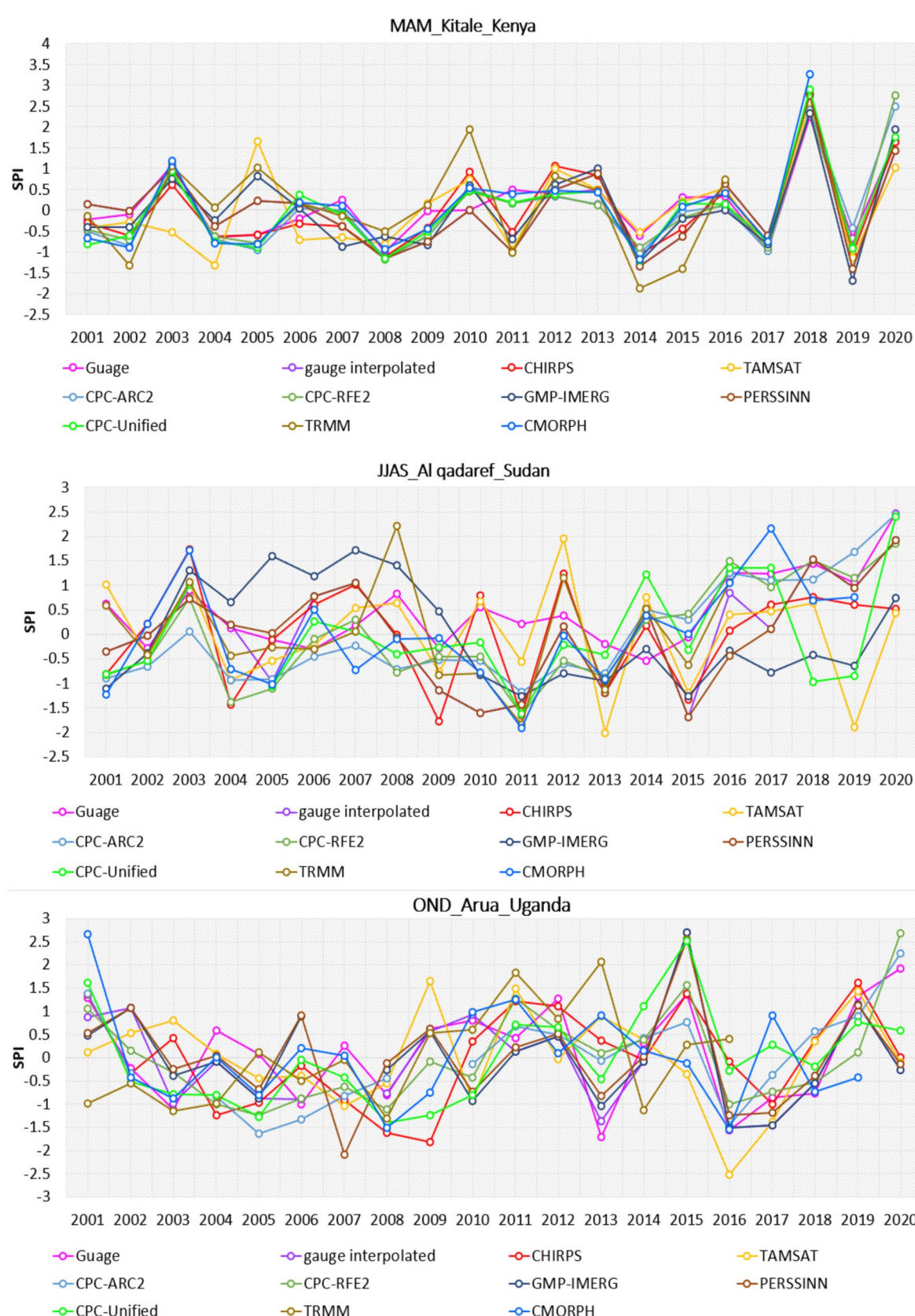


Fig. 13 Show the degree of agreement between the gauge, interpolated gauge, and 9 SRE in simulating the patterns of extreme rainfall events over Kitale in Kenya, Al Qadaref in Sudan, and Arua in Uganda

Al Qadaref in Sudan, and Arua in Uganda. This serves as an example summarizing the patterns of SPI for 105 rain gauges in the IGAD region. The results show that SREs performance varies significantly between seasons, and detecting extreme rainfall events like floods and droughts is a challenge for most satellite products. However, products with higher temporal resolution, such as CMORPH RT V0, CPC RFEv2, GPM-IMERG, CHIRPS v2.0, and CPC ARC2, tend to capture these events more accurately in some years. All 9 SREs products show biases, either underestimating or overestimating extreme rainfall events. There is yearly variation in the performance of 9 SREs between countries and sub-regions within countries. The 9 SREs estimate rainfall more accurately over the highlands of western Kenya compared to ASALs in the north and east, especially in the recent 5 years (Fig. 13a). SREs tend to show larger errors due to the weak signal of light rainfall in dry areas. Variation in SREs sensor characteristics, inputs such as TIR, PMW, and blending algorithms, topography, and rainfall regimes such as convective and stratiform are the main factors affecting the reliability of estimates (Palharini et al. 2020). The interplay of these inputs determines how well satellite precipitation estimates perform in East Africa. Products like CMORPH RT V0, CHIRPS CPC RFEv2, and GPM-IMERG, which blend satellite data with ground station data, often perform better in capturing fine-scale spatial and temporal variations in rainfall compared to TAMSAT v3.1, which uses TIR as inputs (Dinku et al. 2018a, b). Localized mesoscale phenomena weather systems such as thunderstorms and squall lines, mesoscale convective systems, and large-scale phenomena such as tropical cyclones, extratropical cyclones, monsoons, ENSO, and the Indian Ocean Dipole, and localized variability in rainfall intensity significantly influence the performance of SREs in capturing extreme events such as floods and droughts (Barry & Carleton 2010). All 9 SREs perform poorly in Sudan and Uganda during JJAS (Fig. 13b) and OND season (Fig. 13c). This may be attributed to the dynamic movement of the Intertropical Convergence Zone (ITCZ) north and south of the equator, which creates seasonal variability in rainfall, timing, and intensity of rainy seasons within short time frames and across regions (Liu et al. 2020). Infrared-based satellite systems often overestimate rainfall by focusing on cloud-top temperatures in ITCZ regions, leading to false alarms for extreme rainfall events. The ITCZ's response to ENSO and IOD events influences the accuracy of satellite rainfall estimates during climate-driven extremes like floods or droughts (Palmer et al. 2023). The interaction between the ITCZ and East Africa's topography enhances localized rainfall extremes (Oettli & Camberlin 2005), which may be missed or underestimated by lower-resolution satellite sensors. However, the patterns of SPI over Kitale, Al Qadaref, and Arua provide insight on extreme rainfall events and show the importance of SREs

over East Africa. Improvements in satellite technology, algorithms, and data assimilation are expected to enhance the accuracy of these estimates in the future.

4 Summary and conclusions

Satellite precipitation (rainfall) products have become increasingly valuable for climate service delivery in recent years, especially in Africa, where the number of synoptic stations has been decreasing over time. This work gives a detailed long-term comparison and evaluation of nine (9) satellite rainfall estimates (SREs) from 2001 to 2020. The nine SREs employed in this study are CHIRPS v2.0, TAMSAT v3.1, NOAA-CPC ARC2, CPC version 6 data, NOAA-CPC RFEv2, PERSIANN-CDR, CMORPH RT V0.x BLD, GPM-IMERG V06, and TRMM 3B42 v7. These SREs were evaluated using both the 105-rain gauge and spatially interpolated products in regional and five potential agricultural sub-regions in the IGAD region of Eastern Africa. The 105 rain gauge observations were spatially interpolated based on coordinates (longitude and latitude). The extracted values from these interpolated gauges demonstrate clear one-to-one relationships and patterns. The spatial total rainfall and annual cycle results indicated that all SREs exhibit similar patio-temporal patterns over most parts of IGAD region. The results from different validation techniques employed in this study show that a single metric validation approach such as CC, Pbias, ME, RMSE, NSE, categorical metrics (POD, POFD, FAR, CSI, HSS), and volumetric metrics (MQB, MQE, VHI, QPOD, VFAR, QFAR, VMI, and VCSI) cannot accurately reflect the best performance of SREs over any part of the region. Various statistical metrics should be utilized to evaluate the performance of rainfall, especially in regions with complex topography, such as mountains, valleys, plateaus and varying climatic zones. Despite the fact that the majority of the datasets were found to be statistically similar, CMORPH emerged as the best-performing SRE in the IGAD region of Eastern Africa, followed by CHIRPS v2.0, CPC-RFEv2, and GPM-IMERG, while TAMSAT and TRMM were ranked the least. The nine SRE products underestimated the rainfall patterns throughout the region. The performance of SREs is much better in highlands and mountainous regions compared to arid and semi-arid lands (ASALs). Despite the differences in temporal resolution, number of rain gauges, and distribution, as well as uncertainty related to interpolation, the rain gauge interpolated dataset is the best option for climate services in the IGAD region of Eastern Africa. It is important to note that the given results are valid for the SRE products that were used in this study between 2001 and 2020 for each 105-rain gauge extracted based on coordinates in the IGAD region, not each grid. Different outcomes may be reached in different time

frames. Also, if the effect of the rain gauge utilized in merging with satellite products is eliminated, the rated performance of SREs as well as geographical areas may change. The low resolution of some SRE products restricts their applications in climate services. The variation in performance of different SREs may be due to uncertainty related to different sensor limitations, retrieval algorithms, cloud microphysics and rainfall characteristics, surface and environmental conditions, validation and distribution of rain gauge, data processing and integration, climate and seasonal variability. The findings of this study support the use of rain gauges, interpolated rain gauge products supplemented by SREs products for accurate and timely climate services in the IGAD region of Eastern Africa.

Acknowledgements This work is part of a PhD work at the University of Nairobi, Kenya, Faculty of Science & Technology, Department of Earth & Climate Sciences. Also, the author wishes to acknowledge all Sources of datasets used in this study (CHIRPS v2.0 from University of Santa Barbara (UCSB), TAMSAT from Reading University, CPC V6.0, ARC 2, CMORPH, RFE2 from NOAA, TRMM and GPM IMERG from NASA, PERSIANN from University of Arizona) for archiving and open access to the datasets.

Author contributions The idea and execution of the study were jointly developed by all of the authors. Paulino Omoj was responsible for preparing the materials, collecting the data, analyzing, and manuscript's initial draft. Josiah M. Kinama, Christopher Oludhe, and Nzioka J. Muthama supervised all stages of manuscript. Zachary Atheru and Guleid Artan reviewed and secured funding for open access publication. Each author provided feedback on an earlier draft of the manuscript. The final manuscript was reviewed and approved by all writers.

Funding We would like to express our gratitude to Intra-ACP Climate Services and Related Applications (ClimSA) for their assistance, which allowed us to publish this study as open access through the support to the IGAD Climate Prediction and Application Center (ICPAC).

Data availability You can request access to the secondary datasets that have been generated during the analysis. All nine (9) of the satellite products' main datasets are freely available online.

Code availability We used Climate Data Tool (CDT) based R-Packages.

Declarations

Declarations I affirm that the content presented in this article is all my own and has not been published elsewhere. In compliance with the standards set by the University of Nairobi, I have appropriately cited and recognized any instances where the work of others or myself has been utilized.

Conflict of interest All authors declare no competing interests.

Consent to participate All authors consent to participate.

Consent for publication All authors consent to publish this work.

Open Access This article is licensed under a Creative Commons Attribution-NonCommercial-NoDerivatives 4.0 International License, which permits any non-commercial use, sharing, distribution and

reproduction in any medium or format, as long as you give appropriate credit to the original author(s) and the source, provide a link to the Creative Commons licence, and indicate if you modified the licensed material. You do not have permission under this licence to share adapted material derived from this article or parts of it. The images or other third party material in this article are included in the article's Creative Commons licence, unless indicated otherwise in a credit line to the material. If material is not included in the article's Creative Commons licence and your intended use is not permitted by statutory regulation or exceeds the permitted use, you will need to obtain permission directly from the copyright holder. To view a copy of this licence, visit <http://creativecommons.org/licenses/by-nc-nd/4.0/>.

References

- Alexandersson H, Moberg A (1997) Homogenization of swedish temperature data. part I: homogeneity test for linear trends. *Int J Climatol* 17:25–34
- Anyah RO, Qiu W (2012) Characteristic 20th and 21st century precipitation and temperature patterns and changes over the Greater Horn of Africa. *Int J Climatol*. <https://doi.org/10.1002/joc.2270>
- Awange JL, Ferreira VG, Forootan E, Khandu K, Andam-Akorful SA, Agutu NO, He XF (2016) Uncertainties in remotely sensed precipitation data over Africa. *Int J Climatol* 36(1):303–323. <https://doi.org/10.1002/joc.4346>
- Ayehu GT, Tadesse T, Gessesse B, Dinku T (2018) Validation of new satellite rainfall products over the Upper Blue Nile Basin, Ethiopia. *Atmos Meas Tech* 11(4):1921–1936. <https://doi.org/10.5194/amt-11-1921-2018>
- Barry, R. G., & Carleton, A. M. (2010). Synoptic systems. *Synoptic and Dynamic Climatology*, 40–89. https://doi.org/10.4324/9780203218181_chapter_6
- Chen S, Hong Y, Cao Q, Kirstetter PE, Gourley JJ, Qi Y, Zhang J, Howard K, Hu J, Wang J (2013) Performance evaluation of radar and satellite rainfalls for Typhoon Morakot over Taiwan: Are remote-sensing products ready for gauge denial scenario of extreme events? *J Hydrol* 506:4–13. <https://doi.org/10.1016/j.jhydrol.2012.12.026>
- Chen H, Yong B, Qi W, Wu H, Ren L, Hong Y (2020) Investigating the evaluation uncertainty for satellite precipitation estimates based on two different ground precipitation observation products. *J Hydrometeorol* 21(11):2595–2606. <https://doi.org/10.1175/JHM-D-20-0103.1>
- Crow WT, Van Den Berg MJ (2010) An improved approach for estimating observation and model error parameters in soil moisture data assimilation. *Water Resour Res* 46(12):1–12. <https://doi.org/10.1029/2010WR009402>
- Dinku T, Ceccato P, Connor SJ (2011a) Challenges of satellite rainfall estimation over mountainous and arid parts of east africa. *Int J Remote Sens* 32(21):5965–5979. <https://doi.org/10.1080/01431161.2010.499381>
- Dinku T, Ceccato P, Connor SJ (2011b) Challenges of satellite rainfall estimation over mountainous and arid parts of east africa. *Int J Remote Sens* 32(21):5965–5979. <https://doi.org/10.1080/01431161.2010.499381>
- Dinku T, Hailemariam K, Maidment R, Tarnavsky E, Connor S (2014) Combined use of satellite estimates and rain gauge observations to generate high-quality historical rainfall time series over Ethiopia. *Int J Climatol*. <https://doi.org/10.1002/joc.3855>
- Dinku T, Funk C, Peterson P, Maidment R, Tadesse T, Gadain H, Ceccato P (2018a) Validation of the CHIRPS satellite rainfall estimates over eastern Africa. *Q J R Meteorol Soc* 144(August):292–312. <https://doi.org/10.1002/qj.3244>

- Dinku T, Funk C, Peterson P, Maidment R, Tadesse T, Gadaun H, Ceccato P (2018b) Validation of the CHIRPS satellite rainfall estimates over eastern Africa. *Q J R Meteorol Soc* 144(August):292–312. <https://doi.org/10.1002/qj.3244>
- Dinku T, Faniriantsoa R, Islam S, Nsengiyumva G, Grossi A (2022) The climate data tool: enhancing climate services across Africa. *Front Clim* 3(February):1–16. <https://doi.org/10.3389/fclim.2021.787519>
- Farah Hersi M, Akinola AO (2024) IGAD and Multilateral Security in the Horn of Africa. *IGAD and Multilateral Security in the Horn of Africa*. <https://doi.org/10.1007/978-3-031-51548-4>
- Funk C, Nicholson SE, Landsfeld M, Klotter D, Peterson P, Harrison L (2015a) The Centennial Trends Greater Horn of Africa precipitation dataset. *Scientific Data*. <https://doi.org/10.1038/sdata.2015.50>
- Funk C, Peterson P, Landsfeld M, Pedreros D, Verdin J, Shukla S, Husak G, Rowland J, Harrison L, Hoell A, Michaelsen J (2015b) The climate hazards infrared precipitation with stations - A new environmental record for monitoring extremes. *Scientific Data*. <https://doi.org/10.1038/sdata.2015.66>
- Herman A, Kumar VB, Arkin PA, Kousky JV (1997) Objectively determined 10-day African rainfall estimates created for famine early warning systems. *Int J Remote Sens* 18(10):2147–2159. <https://doi.org/10.1080/014311697217800>
- Hou, A. Y., Skofronick-Jackson, G., Kummerow, C. D., & Shepherd, J. M. (2008). Global precipitation measurement. In *Precipitation: Advances in Measurement, Estimation and Prediction*. https://doi.org/10.1007/978-3-540-77655-0_6
- Huffman GJ, Adler RF, Bolvin DT, Gu G, Nelkin EJ, Bowman KP, Hong Y, Stocker EF, Wolff DB (2007) The TRMM Multisatellite Precipitation Analysis (TMPA): Quasi-global, multiyear, combined-sensor precipitation estimates at fine scales. *J Hydroeteorol* 8(1):38–55. <https://doi.org/10.1175/JHM560.1>
- Joyce RJ, Janowiak JE, Arkin PA, Xie P (2004) CMORPH: A method that produces global precipitation estimates from passive microwave and infrared data at high spatial and temporal resolution. *J Hydrometeorol*. [https://doi.org/10.1175/1525-7541\(2004\)005%3c0487:CAMTPG%3e2.0.CO;2](https://doi.org/10.1175/1525-7541(2004)005%3c0487:CAMTPG%3e2.0.CO;2)
- Kawanishi T, Sezai T, Ito Y, Imaoka K, Takeshima T, Ishido Y, Shibusawa A, Miura M, Inahata H, Spencer RW (2003) The Advanced Microwave Scanning Radiometer for the Earth Observing System (AMSR-E), NASDA's contribution to the EOS for global energy and water cycle studies. *IEEE Trans Geosci Remote Sens* 41(2):184–194. <https://doi.org/10.1109/TGRS.2002.808331>
- Kumah KK, Maathuis BHP, Hoedjes JCB, Su Z (2022) Near real-time estimation of high spatiotemporal resolution rainfall from cloud top properties of the MSG satellite and commercial microwave link rainfall intensities. *Atmos Res* 279:106357
- Kumar S, Castillo-Velarde CD, Flores Rojas JL, Moya-Álvarez A, Martínez Castro D, Srivastava S, Silva Y (2020) Precipitation structure during various phases the life cycle of precipitating cloud systems using geostationary satellite and space-based precipitation radar over Peru. *Giscience & Remote Sensing* 57(8):1057–1082. <https://doi.org/10.1080/15481603.2020.1843846>
- Levizzani, V., Kidd, C., Kirschbaum, D. B., Kummerow, C. D., Nakamura, K., & Turk, J. F. (2020). Satellite Precipitation Measurement. In *Satellite Precipitation Measurement, Volume 1* (Vol. 67). <http://link.springer.com/https://doi.org/10.1007/978-3-030-24568-9>
- Liu C, Liao X, Qiu J, Yang Y, Feng X, Allan RP, Cao N, Long J, Xu J (2020) Observed variability of intertropical convergence zone over 1998–2018. *Environ Res Lett* 15(10):104011. <https://doi.org/10.1088/1748-9326/aba033>
- Maggioni, V., Massari, C., & Kidd, C. (2022). Chapter 13 - Errors and uncertainties associated with quasiglobal satellite precipitation products (S. B. T.-P. S. Michaelides (ed.); pp. 377–390). Elsevier. <https://doi.org/10.1016/B978-0-12-822973-6.00023-8>
- Maidment RI, Grimes DIF, Allan RP, Greatrex H, Rojas O, Leo O (2013) Evaluation of satellite-based and model re-analysis rainfall estimates for Uganda. *Meteorol Appl*. <https://doi.org/10.1002/met.1283>
- Murray V, Ebi KL (2012) IPCC Special Report on Managing the Risks of Extreme Events and Disasters to Advance Climate Change Adaptation (SREX). *J Epidemiol Commun Health*. <https://doi.org/10.1136/jech-2012-201045>
- Ndiwa, J. (2015). *Modelling Aerosol-Cloud-Precipitation Interactions For Weather Modification In East Africa*. June.
- Ngoma H, Wen W, Ojara M, Ayugi B (2021) Assessing current and future spatiotemporal precipitation variability and trends over Uganda, East Africa, based on CHIRPS and regional climate model datasets. *Meteorol Atmos Phys* 133(3):823–843. <https://doi.org/10.1007/s00703-021-00784-3>
- Nicholson SE, Klotter DA (2021) Assessing the reliability of satellite and reanalysis estimates of rainfall in equatorial Africa. *Remote Sensing* 13(18):3609. <https://doi.org/10.3390/rs13183609>
- Novella NS, Thiaw WM (2013) African rainfall climatology version 2 for famine early warning systems. *J Appl Meteorol Climatol*. <https://doi.org/10.1175/JAMC-D-11-0238.1>
- Nsengiyumva P (2019) African mountains in a changing climate: Trends, impacts, and adaptation solutions. *Mt Res Dev* 39(2):P1–P8. <https://doi.org/10.1659/MRD-JOURNAL-D-19-00062.1>
- Oettli P, Camberlin P (2005) Influence of topography on monthly rainfall distribution over East Africa. *Climate Res*. <https://doi.org/10.3354/cr028199>
- Oloo JO, Omondi P (2017) Strengthening local institutions as avenues for climate change resilience. *Int J Disast Resil Environ*. <https://doi.org/10.1108/IJDRBE-12-2013-0047>
- Omay PO, Muthama NJ, Oludhe C, Kinama JM, Artan G, Atheru Z (2023) Evaluation of CMIP6 historical simulations over IGAD region of Eastern Africa. *Discov Environ*. <https://doi.org/10.1007/s44274-023-00012-2>
- Omiti JM (2013) Mapping of non-wood forest products (NWFP) and minerals appropriate for artisanal mining for development in the arid and semiarid areas of the IGAD Region. In INTERGOVERNMENTAL AUTHORITY ON DEVELOPMENT (IGAD). <https://doi.org/10.1002/ejoc.201200111>
- Ongoma V, Chen H (2017) Temporal and spatial variability of temperature and precipitation over East Africa from 1951 to 2010. *Meteorol Atmos Phys*. <https://doi.org/10.1007/s00703-016-0462-0>
- Ongoma V, Chena H, Gaoa C (2018) Projected changes in mean rainfall and temperature over east Africa based on CMIP5 models. *Int J Climatol*. <https://doi.org/10.1002/joc.5252>
- Palharini RSA, Vila DA, Rodrigues DT, Quispe DP, Palharini RC, de Siqueira RA, de Sousa Afonso JM (2020) Assessment of the extreme precipitation by satellite estimates over South America. *Remote Sensing* 12(13):1–23. <https://doi.org/10.3390/rs12132085>
- Palmer PI, Wainwright CM, Dong B, Maidment RI, Wheeler KG, Gedney N, Hickman JE, Madani N, Folwell SS, Abdo G, Allan RP, Black ECL, Feng L, Gudoshava M, Haines K, Huntingford C, Kilavi M, Lunt MF, Shaaban A, Turner AG (2023) Drivers and impacts of Eastern African rainfall variability. *Nat Rev Earth Environ* 4(4):254–270. <https://doi.org/10.1038/s43017-023-00397-x>
- Petropoulos, G. P., & Islam, T. (2017). Remote sensing of hydrometeorological hazards. In *Remote Sensing of Hydrometeorological Hazards*. <https://doi.org/10.1201/b20993>
- Romilly TG, Gebremichael M (2011) Evaluation of satellite rainfall estimates over Ethiopian river basins. *Hydrol Earth Syst Sci*. <https://doi.org/10.5194/hess-15-1505-2011>

- Schwartz, P. R. (2004). *Future Directions in the Equities of Ocean*. 38(2), 109–120.
- Smith, E. A., Asrar, G., Furuhama, Y., Ginati, A., Mugnai, A., Nakamura, K., Adler, R. F., Chou, M.-D., Desbois, M., Durning, J. F., Entin, J. K., Einaudi, F., Ferraro, R. R., Guzzi, R., Houser, P. R., Hwang, P. H., Iguchi, T., Joe, P., Kakar, R., ... Zhang, W. (2007). *International Global Precipitation Measurement (GPM) Program and Mission: An Overview BT - Measuring Precipitation From Space: EURAINSAT and the Future* (V. Levizzani, P. Bauer, & F. J. Turk (eds.); pp. 611–653). Springer Netherlands. https://doi.org/10.1007/978-1-4020-5835-6_48
- Song S, Yan X (2022) Evaluation of events of extreme temperature change between neighboring days in CMIP6 models over China. *Theoret Appl Climatol* 150(1–2):53–72. <https://doi.org/10.1007/s00704-022-04142-0>
- Sorooshian S, Hsu KL, Gao X, Gupta HV, Imam B, Braithwaite D (2000) Evaluation of PERSIANN system satellite-based estimates of tropical rainfall. *Bull Am Meteor Soc*. [https://doi.org/10.1175/1520-0477\(2000\)081%3c2035:EOPSS%3e2.3.CO;2](https://doi.org/10.1175/1520-0477(2000)081%3c2035:EOPSS%3e2.3.CO;2)
- Stephens GL, Kummerow CD (2007) The remote sensing of clouds and precipitation from space: A review. *J Atmos Sci* 64(11):3742–3765. <https://doi.org/10.1175/2006JAS2375.1>
- Suri A, Azad S (2024) Optimal placement of rain gauge networks in complex terrains for monitoring extreme rainfall events: a review. *Theoret Appl Climatol* 155(4):2511–2521. <https://doi.org/10.1007/s00704-024-04856-3>
- Sylla, M. B. (2018). Review of meteorological / climate data sharing policy (WMO Resolution 40) to promote their use to support Climate Information Services uptake in the African continent. *Expert Group Meeting on Data Sharing Policy in Africa, July*, 10–11.
- Tarnavsky E, Grimes D, Maidment R, Black E, Allan RP, Stringer M, Chadwick R, Kayitakire F (2014) Extension of the TAMSAT satellite-based rainfall monitoring over Africa and from 1983 to present. *J Appl Meteorol Climatol*. <https://doi.org/10.1175/JAMC-D-14-0016.1>
- Tarnavsky, E., & Bonifacio, R. (2020). *Drought Risk Management Using Satellite-Based Rainfall Estimates BT - Satellite Precipitation Measurement: Volume 2* (V. Levizzani, C. Kidd, D. B. Kirschbaum, C. D. Kummerow, K. Nakamura, & F. J. Turk (eds.); pp. 1029–1053). Springer International Publishing. https://doi.org/10.1007/978-3-030-35798-6_28
- Taylor RG, Todd MC, Kongola L, Maurice L, Nahozya E, Sanga H, Macdonald AM (2013) Evidence of the dependence of groundwater resources on extreme rainfall in East Africa. *Nat Clim Chang*. <https://doi.org/10.1038/nclimate1731>
- Xie H, Li D, Xiong L (2014) Exploring the ability of the Pettitt method for detecting change point by Monte Carlo simulation. *Stoch Env Res Risk Assess* 28(7):1643–1655. <https://doi.org/10.1007/s00477-013-0814-y>

Publisher's Note Springer Nature remains neutral with regard to jurisdictional claims in published maps and institutional affiliations.